Catalysis Today 160 (2011) 11–27

Contents lists available at ScienceDirect

Catalysis Today

journal homepage: www.elsevier.com/locate/cattod

Review

Conductive materials by metal catalyzed polymerization☆

Cristina Della Pina, Ermelinda Falletta, Michele Rossi*

Dipartimento di Chimica Inorganica, Metallorganica e Analitica "L. Malatesta", Università degli Studi di Milano, CNR-ISTM, Via G, Venezian, 21, 20133 Milano, Italy

ARTICLE INFO

Article history:
Available online 23 June 2010

Keywords:
Conductive polymers
Metal catalysis
Polymerization
Clean processes

ABSTRACT

This article reviews the metal catalyzed syntheses of aniline and pyrrole leading to conductive polymers. Considering that these materials are commonly produced via electrochemical or chemical processes, catalytic methods could represent a strategic tool for improved technologies based on the use of clean reagents, such as dioxygen and hydrogen peroxide. The advantage of avoiding either the use of a large amount of reagents or the formation of unsustainable amounts of by-products is highlighted. Beside synthetic and mechanistic aspects of the catalytic preparation of polyaniline and polypyrrole, a critical description of the morphological properties, related to the choice of the catalytic system, is presented.

Contents

1. Introduction

Conductive polymers are emerging materials showing the electronic properties of both metals and semiconductors associated to the mechanic properties of organic macromolecules. Since the first preparation of the highly conducting polyacetylene (PA) in 1977, much efforts have been focused on the synthesis of other organic conducting polymers in particular polyaniline (PANI) and polypyrrole (PPy). At the same time, the great versatility of such materials produced exciting applications in many devices combining optical, electrochemical and conducting properties [1,2]. Polyaniline and polypyrrole are appealing because of their tuneable conductivity and stability in air [3] that allow applications in electronic displays [4], electrode materials [5], molecular electronic circuit elements [6], restoration of data [7], indicators of gasometers [8], and biochemical analysis [9].

The morphology of conducting polymers is an important factor acting a vital influence on characteristics and performance

---

☆ This paper is for a special issue entitled "Heterogeneous Catalysis by Metals: New Synthetic Methods and Characterization Techniques for High Reactivity" guest edited by Jinlong Gong and Robert Rioux.

* Corresponding author.

E-mail address: michele.rossi@unimi.it (M. Rossi).

0920-5861/$ – see front matter © 2010 Elsevier B.V. All rights reserved.
doi:10.1016/j.cattod.2010.05.023

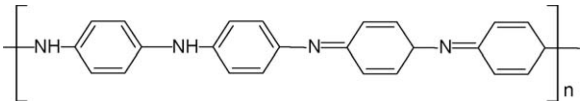

Fig. 1. Polyaniline structure.

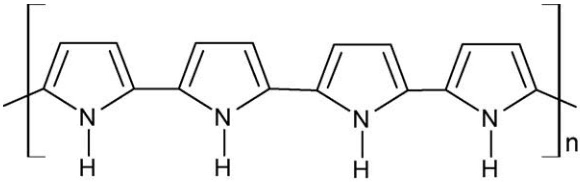

Fig. 2. Polypyrrole structure.

of the material. Unusual geometries of conductive polymers as films, hollow spheres, and nanoparticles, find new applications in many fields, as OLED, drug delivery, materials for absorption and separation. Many sophisticated geometric structures arise either from the synthetic method or from the use of templating agents [10,11]. Therefore, the technology for producing conductive materials embodies the choice of many reagents and the separation of co-products: this consideration highlights the present interest in sustainable chemical processes for the synthesis of high purity products according to a clean technology. Taking into account that conductive polyaniline and polypyrrole are produced mainly by oxidative coupling of the monomers, catalytic processes represent a strategic tool for technologies based on the use of favourite reagents such as dioxygen and hydrogen peroxide. Also the non-oxidative polymerization, as the aryl amination of aryl halides, took advantage from catalysis by metals. The present review displays the state of art of metal-catalyzed syntheses of polyaniline and polypyrrole, along with the properties of derived materials.

2. Structures and electronic properties of polyaniline and polypyrrole

The basic chemical backbones of conducting polyaniline and polypyrrole are shown in Figs. 1 and 2.

Concerning polyaniline, ca. half of the total nitrogen along the chain is in the reduced state (amine, —NH—) and the remaining in the oxidized state (imine, —N=). As a consequence, the configuration of the neighbouring rings is either in a benzenic-like or quinoid-like structure, respectively. The above polyaniline chain, normally called *emeraldine*, can therefore be represented as a mixture of amine-benzenic and imine-quinoid segments [12]. Many other structures are known where nitrogen is in the completely reduced state, *leucoemeraldine* form (Fig. 3), or in the fully oxidized state, *pernigraniline* form (Fig. 4). Between these two limits, a very large number of intermediate states could exist: however, only a few of them are stable, as *protoemeraldine* (Fig. 5), and *nigraniline* (Fig. 6) [13].

The *emeraldine* form of PANI contains an equal number of imine and amine nitrogen atoms (Fig. 1), the former being more basic thus undergoing an easier protonation compared with the amine sites, which are protonated only at high acid concentrations [14]. The secondary amine group (–NH–) in pyrrole is even less basic than the corresponding group in aliphatic compounds. The acid–base transition in the polymers is responsible for the strong change of their conductivities: deprotonation of PANI lowers the conductivity from 4.4 to 6.0×10^{-11} S cm^{-1} [15], and in the case of polypyrrole from 0.5 to 3.2×10^{-9} S cm^{-18} [16].

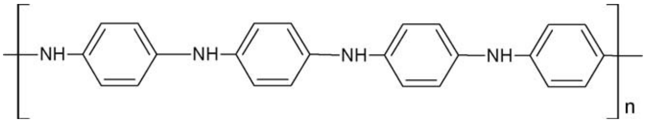

Fig. 3. Leucoemearldine structure.

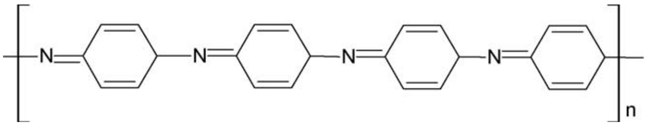

Fig. 4. Pernigraniline structure.

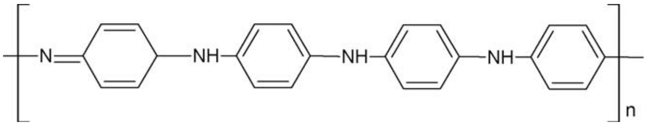

Fig. 5. Protoemeraldine structure.

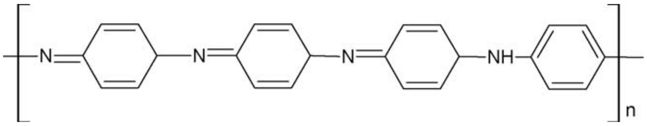

Fig. 6. Nigraniline structure.

The origin of conductivity is explained by the ability of the polymer to form polarons, cation radicals (Fig. 7) [17].

The presence of extensive conjugation in these materials reduces the energy difference between the HOMO/valence and LUMO/conduction bands (i.e. the band gap), essentially making them small band gap semiconductors. However, this reduction in the band gap is not sufficient to achieve appreciable electrical conductivities. The highest observed conductivities are usually obtained in doped polymers where dopants induce perturbations in the electronic structure, resulting in the formation of charge carriers (electrons or "holes" depending on the type of dopant). These features of conducting polymers (low band gap, dopant induced charge carriers and conductivities intermediate between insulators and metals) allow a parallel with physical models applied to inorganic semiconductors [18].

Organic conducting polymers typically exhibit some common characteristics. Owing to their extensive conjugation, they are conformationally rigid molecules. Most conducting polymers are insoluble in the common organic solvents (polyaniline displays a limited solubility in *m*-cresol, 2-pyrrolidinone and concentrated sulfuric acid, whereas no report on polypyrrole solubility exists). Organic conducting polymers also tend to be infusible (they do not melt). Additionally, these materials are usually brittle and have

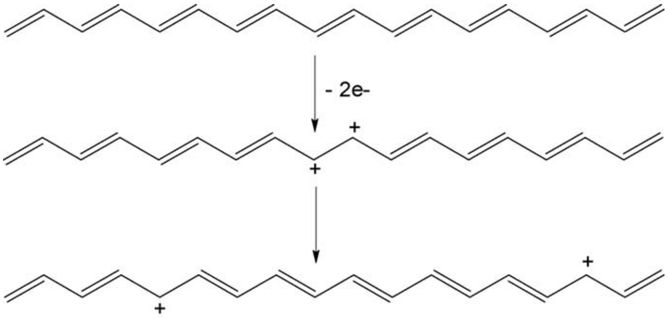

Fig. 7. Illustration of the formation of two charged solitons on a chain of *trans*-polyacetylene.

poor mechanical properties. All of these properties are presumably related to energetically favourable interactions of the π-systems of proximal chains which are stronger than those of polymer with solvent, thus explaining the insolubility and the infusibility. Moreover, the humble mechanical properties due to potential fracture points derive from the anisotropic character of the intermolecular π-system interactions producing amorphous bulk material. All these aspects lead to the difficult characterization by most conventional methods [19].

Nevertheless, polyaniline and polypyrrole are of high interest due to their outstanding properties as tuneable conductivity and stability in air [3].

3. Standard preparation methods of conducting organic polymers: polyaniline and polypyrrole

A comprehensive review of the general properties and mechanisms of electrochemical polymerization of pyrrole can be found in [20]. Conducting organic polymers can be prepared by numerous methods and a short description of the main synthetic routes, the electrochemical and chemical polymerization, is presented in Sections 3.1 and 3.2 while this review is mainly focused on the metal-promoted oxidative polymerization reported in Section 4.

The properties of recently developed mixed polymers as poly(aniline-*co*-pyrrole) [21] are not discussed in the present paper.

3.1. Electrochemical synthesis

The electrochemical method ensures the control of film thickness and morphology. Films of electronically conducting polymers are generally deposited onto a supporting electrode surface by anodic oxidation (electropolymerization) of the corresponding monomer in the presence of an electrolyte solution [20]. Different techniques can be used including potentiostatic (constant potential), galvanostatic (constant current) and potentiodynamic (potential scanning, i.e. cyclic voltammetry) methods [22].

The choice of the solvent and electrolyte requires particular attention because they should be stable at the oxidation potential. Organic solvents like acetonitrile or propylene carbonate have a large potential window [23], and high permittivity, which allow a good dissociation of the electrolyte and thus a good ionic conductivity. Since pyrrole has a relatively low oxidation potential, its polymerization in aqueous medium is allowed [24]. The oxidation starts with the formation of the radical monomeric cation which couples with other monomers present in solution to form firstly oligomeric products and then the polymer. The extended conjugation in the polymer results in a lowering of the oxidation potential compared to the monomer. The synthesis and doping of the polymer are generally done simultaneously: the doping anion is incorporated into the polymer to ensure the electrical neutrality of the film and, at the end of the reaction, a polymeric film of controllable thickness is formed. The anode is made by a variety of materials including platinum, gold, glassy carbon, and tin or indium–tin oxide (ITO) coated glass [25]. The electropolymerization is generally achieved by potentiostatic (constant potential) or galvanostatic (constant current) methods. These techniques are particularly suitable for mechanistic investigation (nucleation and the macroscopic growth). Potentiodynamic techniques, such as cyclic voltammetry, correspond to a repetitive triangular potential waveform applied at the surface of the electrode. The latter method has been mainly used to obtain information about the redox processes involved in the early stages of the polymerization reaction, and to examine the electrochemical behaviour of the polymeric film after deposition [25]. The electropolymerization mechanism is still a research topic of relevant interest. In this context, the contrasting interpretation of pyrrole polymerization is emblematic. According to Funt and Diaz [26,27] and supported by Waltman and Bargon [28,29] the pyrrole activation occurs through electron transfer from the monomer forming a radical cation-rich solution near the electrode in several steps.

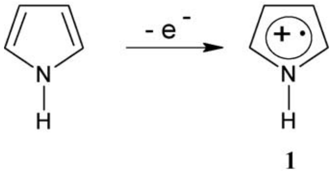

Scheme 1.

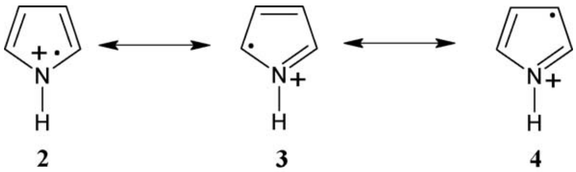

Scheme 2.

- Step 1: The first step implies the oxidation of monomer R at the surface of the electrode to form the cation radical $R\bullet^+$ (**1**), as shown in Scheme 1.

The several resonance forms of this cation are represented in Scheme 2.

The monomeric radical cation can undergo different reactions depending on its reactivity:

- If $R\bullet^+$ is relatively stable, it can diffuse into the solution and react to form soluble products with low molecular weights.
- If $R\bullet^+$ is very unstable, it can react rapidly near the electrode with the solvent or with the doping anion forming soluble products of low molecular weight.
- Between these two extremes, $R\bullet^+$ can undergo a coupling reaction (step 2).

- Step 2: The radical cation $R\bullet^+$, having a great, unpaired electron density in the α-position, dimerizes *via* the resonance form **3**, as shown in Scheme 3. The coupling of two radicals occurs *via* bond formation at the α-positions leading to the dihydromer dication **5**.
- Step 3: The loss of two protons forms the aromatic dimer **6** (stabilization step) shown in Scheme 4.
- Step 4: The polymerization reaction occurs through the oxidation of the dimer **6** to the radical cation **7** (Scheme 5). Since the unpaired electron is now delocalized over two rings, the oxidation potential of **6** is lower than the oxidation potential of the monomer. The dimer **6** is therefore more easily oxidized at the applied potential, which is the oxidation potential of the monomer. Another consequence of this stabilization is that the dimer radical cation becomes less reactive than the monomer.

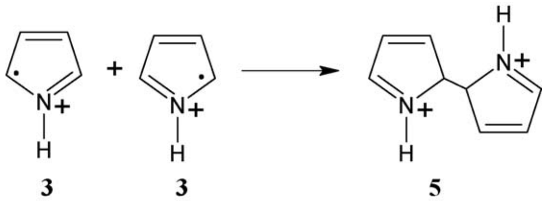

Scheme 3.

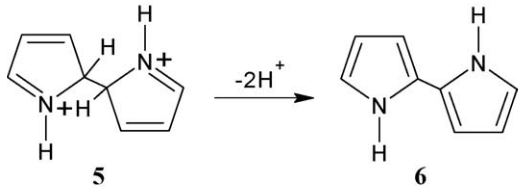

Scheme 4.

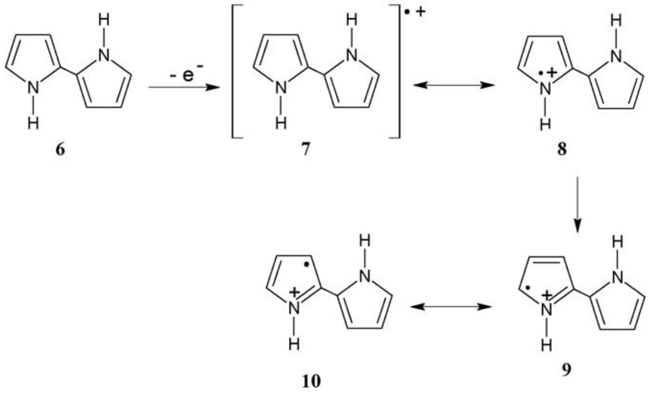

Scheme 5.

The positions 5–5′ are equally the most reactive points and the resonance form **9** is predominant with respect to the other forms.

- Step 5: The resonance form **9** reacts at the position 5 or 5′ with a monomer radical cation **3** to form the trimer dication **11** that deprotonates to give the neutral trimer **12**, as shown in Scheme 6.
- Step 6: The electro-oxidation of **12** gives the radical cation **13** (see Scheme 7).

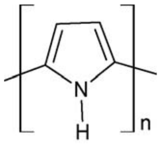

Scheme 8.

The trimer 5–5′ (α-position) and 3–3′ (β-position) positions can undergo coupling reactions with the following oligomers even if the β-positions are sterically inaccessible. The α-coupling will predominate. However, the oligomeric chain, as well as the delocalization of the unpaired electron, increases progressively and the α-coupling will no longer be the only possible coupling. The longer the chain length the higher the number of β-bonds formed. By using XPS, Street has shown that one pyrrole unit every three is affected by structural disorder [30–32]. These β-couplings are responsible for the poor crystal order in polypyrrole. Poly(3,4-dimethylpyrrole), which can only form α-couplings because the β-positions are blocked, does indeed show an improved crystal order.

- Step 7: The propagation proceeds *via* the same sequence: oxidation, coupling, deprotonation until the final polymer product is obtained (see Scheme 8).
- Step 8: The electropolymerization does not give the neutral non-conducting polypyrrole but its oxidized conducting form (doped). Actually, the final polymer chain carries a positive charge every 3–4 pyrrole units, which is counter-balanced by an anion. The structure of the doped polymer is presented in Scheme 9 where A is the electrolyte anion.

Electrochemical film formation is often followed by stoichiometric determination of the number of electrons donated by each molecule. This value is generally found to be between 2 and 2.7, where 2 electrons serve in the film formation and the excess charge is consumed by the polymer oxidation. This number agrees with the number of anions found in the polymer by elementary analysis.

Electron Paramagnetic Resonance (EPR) observations support the existence of a π-type radical [31]. In addition, the elimination of H from the α-position indicated by this mechanism accounts for the observed pH drop of the solution during polymerization. Chronoabsorption studies have shown that the film grows up lin-

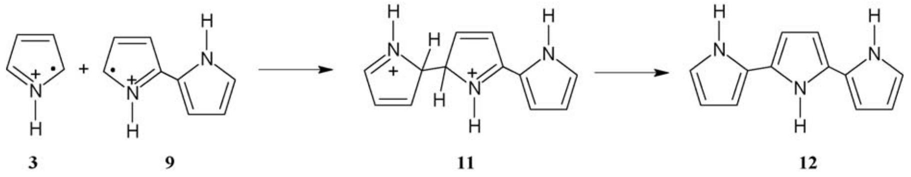

Scheme 6.

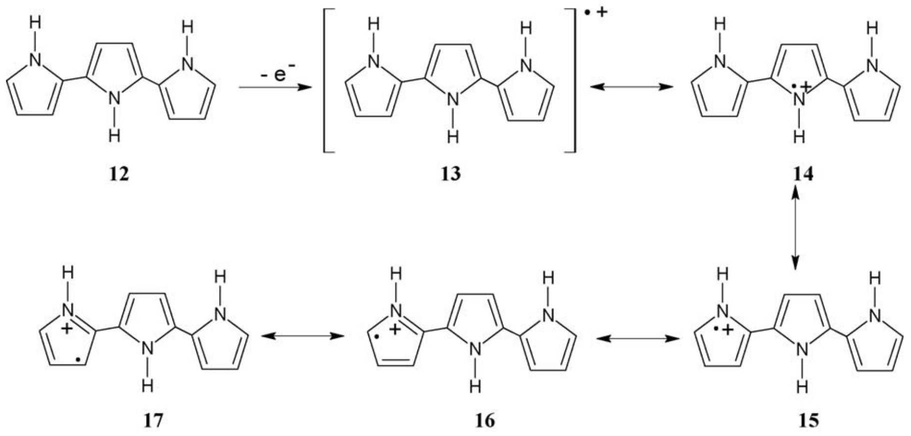

Scheme 7.

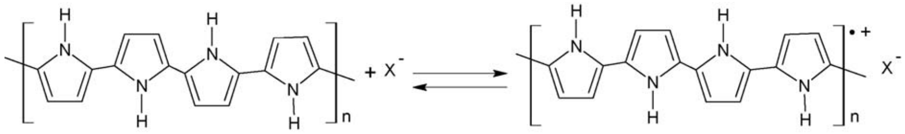

Scheme 9.

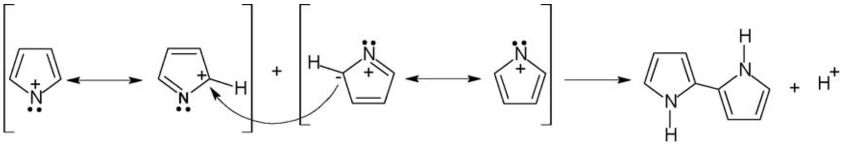

Scheme 10.

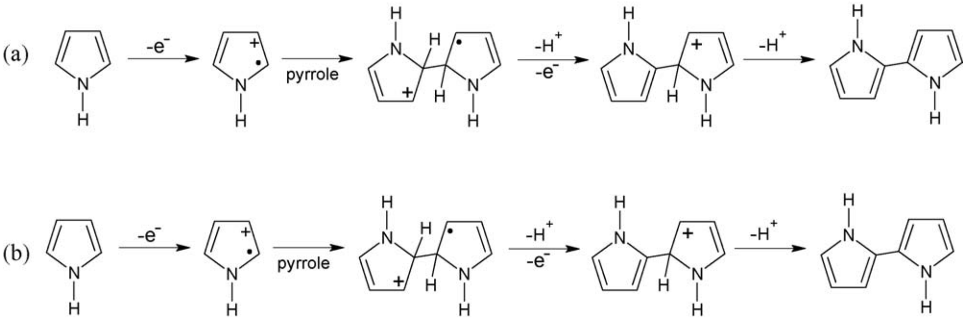

Scheme 11.

early with respect to t and not to $t^{1/2}$. This observation indicates that the rate-determining step during the film growth is the coupling process and not the monomer diffusion towards the electrode [27].

Kim et al. have proposed another mechanism, shown in Scheme 10, where polymerization is initiated by the loss of one proton and two electrons from the pyrrole molecule forming the active intermediate Py^+ [33]. This intermediate undergoes dimerization with a neutral pyrrole molecule and the loss of a second proton. The polymer chain is further extended by the same mechanism (loss of two electrons and coupling).

A quite different "multilayer model", supported by a thorough ellipsometric study, has been proposed by Kim et al. [34].

Accordingly, the polymeric film is deposited in three stages:

1. Initial absorption of the monomer.
2. Formation of a dense polymer from the bidimensionally absorbed monomer and nucleation of low molecular weight polypyrrole molecules in solution.
3. Tridimensional growth layer by layer. In this stage, monomer oxidation occurs more easily on the polymer than on the electrode, as supported by the study of Pletcher and co-workers [35].

A different interpretation was given by Pei and Qian for the initial stage of electropolymerization which supports its occurrence in solution followed by polymer precipitation [36].

Pletcher and co-workers have suggested another mechanism in which the cation radical, formed by the loss of an electron, reacts directly with a neutral molecule giving a cation dimer [35]. The cation dimer then loses a second electron and 2 protons, thus forming the neutral dimer. Satoh et al. have studied this coupling mechanism by comparing it to the classical coupling between two cation radicals [37].

They explained the experimental results by the coupling between a monomer molecule and a cation radical, which corresponds to an aromatic substitution reaction of an electrophile as shown in Scheme 11.

Thus, the coupling reaction (a) and the resulting polymerization are affected by the monomer concentration [38]. However, the conclusion of Satoh concerning the coupling reaction has been challenged by Takakubo who demonstrated, by molecular orbital calculations, that the addition of a cation radical to a neutral molecule is symmetry forbidden and thus requires a high activation energy [39].

Qiu and Reynolds have studied the polymerization of pyrrole by Electrochemical Quartz-Crystal Microbalance (EQCM) in various aqueous electrolytes [40]. Under specific conditions in the presence of ClO_4^-, BF_4^- and PF_6^- electrolytes, three stages are observed during the polymerization process where the number of electrons involved (n) is different. The first and the second stages give n values of 1.60 and 0.12 respectively, whereas the third stage gives a n value of 2.50. This last n value is the one observed in the classical mech-

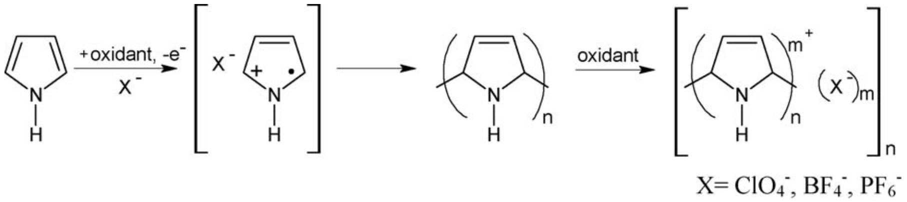

Scheme 12.

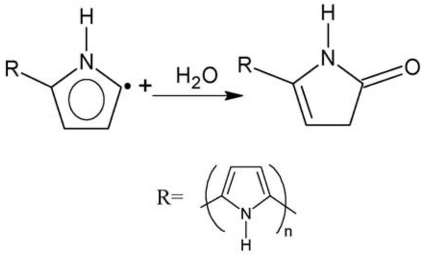

Scheme 13.

anism and so this last stage is representative of Diaz's mechanism. To explain the low *n* numbers and high rates of polymerization in the first two stages, an electrochemically initiated chain polymerization mechanism was proposed, which starts up the formation of the PPy film [40]. This chain polymerization process is predominant with respect to the radical cation coupling during the first two stages of the reaction.

The reaction, presented in Scheme 12, is initiated by the generation of monomer radical cations at the surface of the electrode followed by a rapid growth of the chain and by a low *n* value. The obtained non-conjugated polymer becomes conjugated and takes on the doped polypyrrole form by oxidation at the electrode. Note that this mechanism is only valid in aqueous solution and in the presence of the above cited electrolytes. As explained by the authors, the strong interaction between the solvent (H_2O) and the radical cations, and the anion ability to activate the initiation step enable this type of mechanism. The obtained polymer allows the transfer of cations and anions during the electrochemical switching among the different redox states, unlike the polymers synthesized by radical cation coupling which are only capable of transporting the anions.

The final step in the polymerization is not clear and different hypotheses have been proposed. Funt and Diaz [26,27] believe that the reaction with water, shown in Scheme 13, could be responsible for the polymerization quench.

In contrast, Street [31] believes that the growth of the chain stops because the radical cation becomes relatively unreactive towards the chain propagation or because the reactive chain ends become sterically blocked.

The electrochemical synthesis of polyaniline can be explained using similar schemes.

One of the principal difficulties encountered in the determination of the different stages of the reaction is the rapidity of the polymerization. In addition, the insolubility of polypyrrole coupled with its non-crystalline nature makes structure characterization and physical properties exceedingly difficult.

3.2. *Chemical synthesis*

The oldest and still the most popular route for the preparation of bulk-polyaniline and- polypyrrole is the chemical oxidative polymerization. The optimization of the process has been widely investigated during the past two decades. Several papers devoted to the polymerization in organic solvents have been published [41], but the reaction in aqueous solutions at low pH still remains the most extensively studied one. In this latter case, many inorganic oxidants such as KIO_3, $KMnO_4$, $FeCl_3$, K_2CrO_4, $KBrO_3$, $KClO_3$, $(NH_4)_2S_2O_8$ (APS) have been tested [42–45].

A strong drawback in using these "stoichiometric oxidants" is the formation of a large amount of by-products: in the case of APS, the amount of resulting ammonium sulfate is about 1 kg per kg of organic polymer.

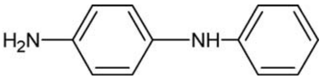

Fig. 8. *N*-4-aminophenylaniline.

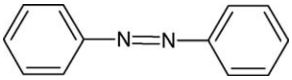

Fig. 9. *Trans*-azobenzene.

Concerning the chemical oxidation of aniline and pyrrole, there are no detailed mechanisms as those reported for the electrochemical polymerization.

It is generally accepted that the first step of the polymerization consists in the formation of the dimeric species *N*-4-aminophenylaniline (Fig. 8), *trans*-azobenzene (Fig. 9) and benzidine (Fig. 10).

Wei et al. have proposed a mechanism of aniline polymerization mainly based on kinetic studies of the electrochemical polymerization of aniline (Scheme 14) [46–49].

According to the authors, the slow step is the oxidation of aniline monomer to form dimeric species i.e. *N*-4-aminophenylaniline (Fig. 8), *trans*-azobenzene (Fig. 9) and benzidine (Fig. 10) as supported by the higher oxidation potential of aniline with respect to the dimers. After formation, the dimers are quickly oxidized thus reacting with the monomer *via* an electrophilic aromatic substitution, followed by further oxidation and deprotonation to afford the trimers. This process is repeated, leading eventually to the formation of PANI.

According to Genies and Lapkowski [50], the oxidation of aniline to the dimer occurs through the nitrenium cation ($C_6H_5NH^+$) which has been experimentally observed by means of electronic absorption spectroscopy. However, considering kinetic and thermodynamic aspects, the authors derived that the oxidation of aniline to the dimer is not the slowest step in the polymerization, but appears to be the step requiring the highest electrochemical potential. Related to these aspects key points of the oxidative polymerization are:

1. What the oxidation potential of the oligomers is dependent on?
2. What does force the oligo- and polyaniline chains to grow up and why does the propagation terminate when the emeraldine oxidation state of PANI has been reached?
3. What are the basic factors determining the "activity" of the growing chain in the monomer addition?

In recent years, Gospodinova et al. have substantially contributed to shed a light into the mechanism [51–60]. Following the *in situ* formation of the intermediates and determining the electrochemical potential at different pH values, the authors proposed the elementary steps of the polymerization process (initiation, propagation and termination).

The proposed mechanism (Scheme 15) was theoretically supported by the Hueckel method [57], taking into account that the electrochemical potential of the redox transition fairly correlates with the difference in the π-electron energy of the oxidized and reduced forms, E_π, of a given conjugated molecule [61]. The authors calculated the E_π of oligoanilines with various numbers of units *n*, the degree of oxidation (number of π-electrons involved in the

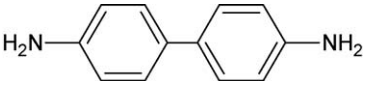

Fig. 10. Benzidine.

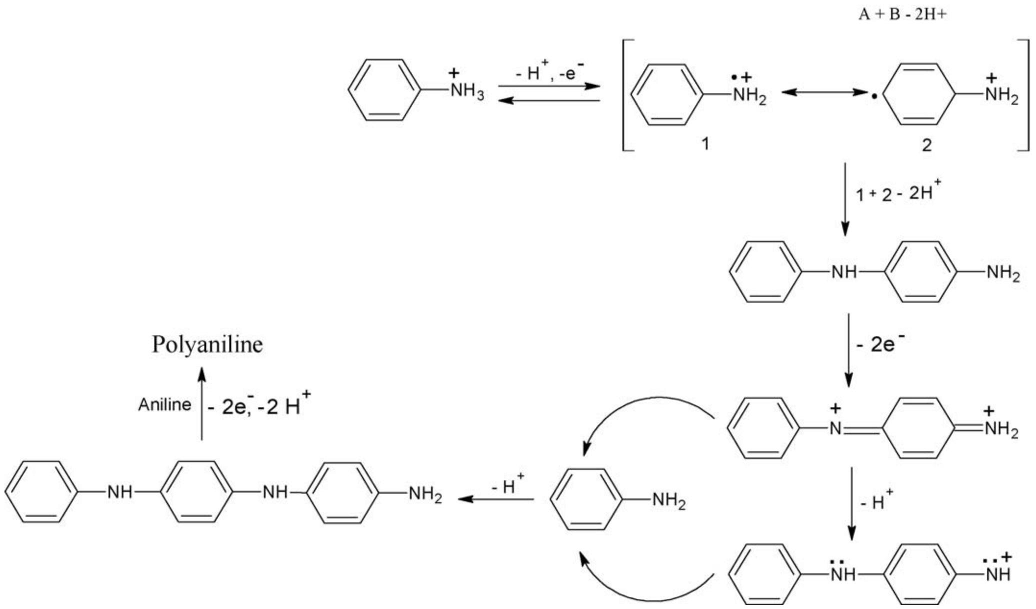

Scheme 14. Mechanism of the aniline polymerization proposed by Wei et al.

redox transition, *m*) and the degree of protonation, with the following assumptions:

1. The basicity of the imine nitrogen atoms is substantially higher than the amine nitrogen one.
2. The oligoanilines with $n > 8$ reproduce to a great extent the characteristics of PANI.

The redox transitions were simulated as processes of electron detachment or acceptance, mainly concerning population of the frontier molecular orbitals. The adopted model gives a relevant description of the formation of a propagating particle.

4. Metal-promoted oxidative polymerization

As above pointed out, one of the most conventional chemical synthesis of polyaniline and polypyrrole is the stoichiometric oxidation which utilizes harsh oxidants (generally APS) and strong mineral acids and producing a relevant amount of by-products [62,63].

A modern approach to large scale productions of conductive polymers suggests the use of environmentally benign processes [45,64–71] where eco-friendly oxidants, as molecular oxygen and hydrogen peroxide, are used [71–77].

From a thermodynamic point of view, the reagent H_2O_2 is advantaged owing to its higher redox potential (1.77 V vs SCE), which is enough for initiating and sustaining aniline polymerization. Moreover, the formation of H_2O as the only reduction product greatly simplifies post-treatments and recycling. Often the oxidation by dioxygen and hydrogen peroxide is a slow process which can be accelerated by the use of a catalyst [67,72,76–82]. In addition, an energetic support can be derived by the use of sonochemical irradiation [78]. Many catalysts have been studied for promoting the oxidative polymerization of aniline and pyrrole, mainly consisting in soluble metal ions in high oxidation states or more complex heterogeneous systems.

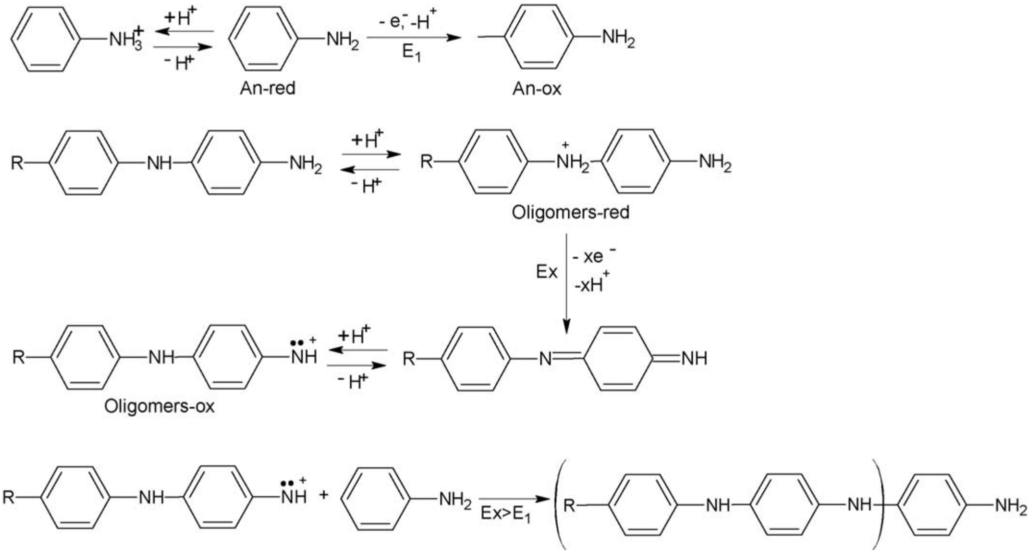

Scheme 15. Mechanism for the aniline polymerization proposed by Gospodinova and Terlemezyan.

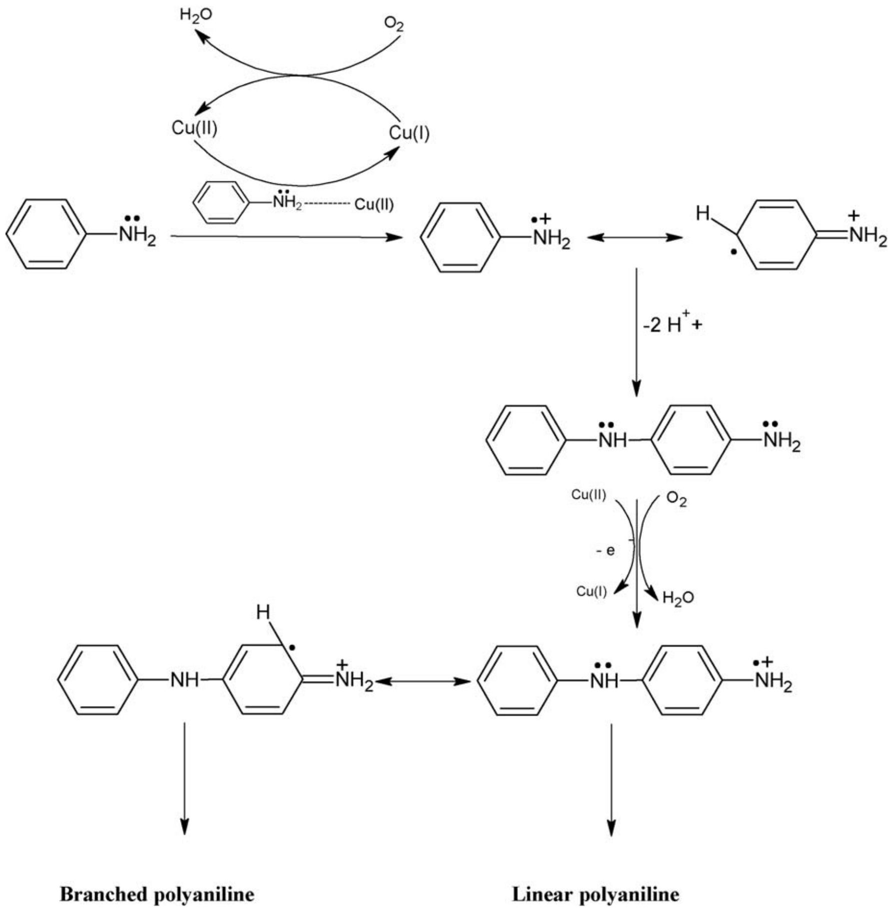

Scheme 16. Suggested mechanism of the copper-catalyzed aniline polymerization.

4.1. Cu-promoted aniline polymerization

In 1994, Toshima et al. reported, for the first time, the catalytic polymerization of aniline and its derivatives using copper (II) salts as a catalyst and molecular oxygen as the oxidant, to obtain polyaniline in the basic form [82]. The polymerization takes place by stirring the aniline solution in the presence of copper(II) ion (50/5, mmol/mmol) in acetonitrile and water (1/1, v/v) under oxygen at room temperature for 24 h. Among copper salts, $CuBr_2$ and $CuCl_2$ resulted to be the most active but the yields were, in any case, low (under 50%). It has been proved that the copper salt does not work as a stoichiometric oxidant but as a true catalyst. The isolated polymers showed characteristics typical of the emeraldine structure, with a small amount of branched structure derived from addition at *ortho*-position. However, after acidification, the electroconductivity resulted to be lower than the expected one, probably because of its amorphous structure. According to spectroscopic investigation, the catalytic polymerization of aniline is supposed to occur through an aniline-copper(II) complex (Scheme 16).

Bicak and Karagoz confirmed the catalytic role of Cu(II) for aniline polymerization in aqueous emulsion producing high molecular weight emeraldine base polymers (23,000–114,000 Da) [66]. Spectroscopic investigations (UV–vis, FT-IR and ^{1}H NMR) showed that the acid-doped PANI had the same structure and similar electronic conductivities (0.067–0.320 S cm^{-1}) of the PANI derived by the conventional persulfate oxidation.

The use of sophisticated copper complexes for the polymerization of aniline has attracted much attention. Dias et al. have reported the synthesis of polyaniline starting from aniline as the reagent, in the presence of HCl as the dopant, H_2O_2 as the oxidant and the copper(II) scorpionate as the catalyst, using different solvents. The best observed yield was ca. 60%. It has been pointed out that the conductivity of the resulting polymer depends strongly on the solvent, following the order acetonitrile > 1:1 acetonitrile–water mixture > water. The polymer prepared using $CuCl_2 \cdot 2H_2O$ catalyst, as a reference, was of relatively poor quality and low conductivity [76].

As previously reported in Section 3.1, the difficult step in aniline polymerization is the oxidation of the monomer to form dimeric species, which are smoothly oxidized to PANI because of their lower oxidation potential [49].

Thus, starting from the preformed aniline dimer, *N*-4-aminophenylaniline, we can strategically improve the polymerization process. In this context, the polymerization of *N*-4-aminophenylaniline has been investigated using hydrogen peroxide as the oxidant and a pyrazolylcopper (II) complex as the catalyst in a mixture 1:1 acetonitrile–water as a solvent [77]. Beside the modest yield of PANI (50%), the need for organic solvents makes this experiment troublesome and far to represent a green process.

Recently, the oxidative polymerization of aniline dimer has been revisited showing that an effective, eco-friendly route to produce polyaniline in the emeraldine conductive form can be performed using metal copper or simple copper compounds, either with O_2 or H_2O_2 as oxidants. It has been outlined the advantage in using aqueous solution instead of acetonitrile, used in previous studies, because this latter behaves as a strong inhibitor [72].

Blank tests have shown that the spontaneous oxidation by O_2 is weak (13% yield) while H_2O_2 allows a higher, but incomplete, polymerization (43% yield). On adding acetonitrile as a co-solvent, the

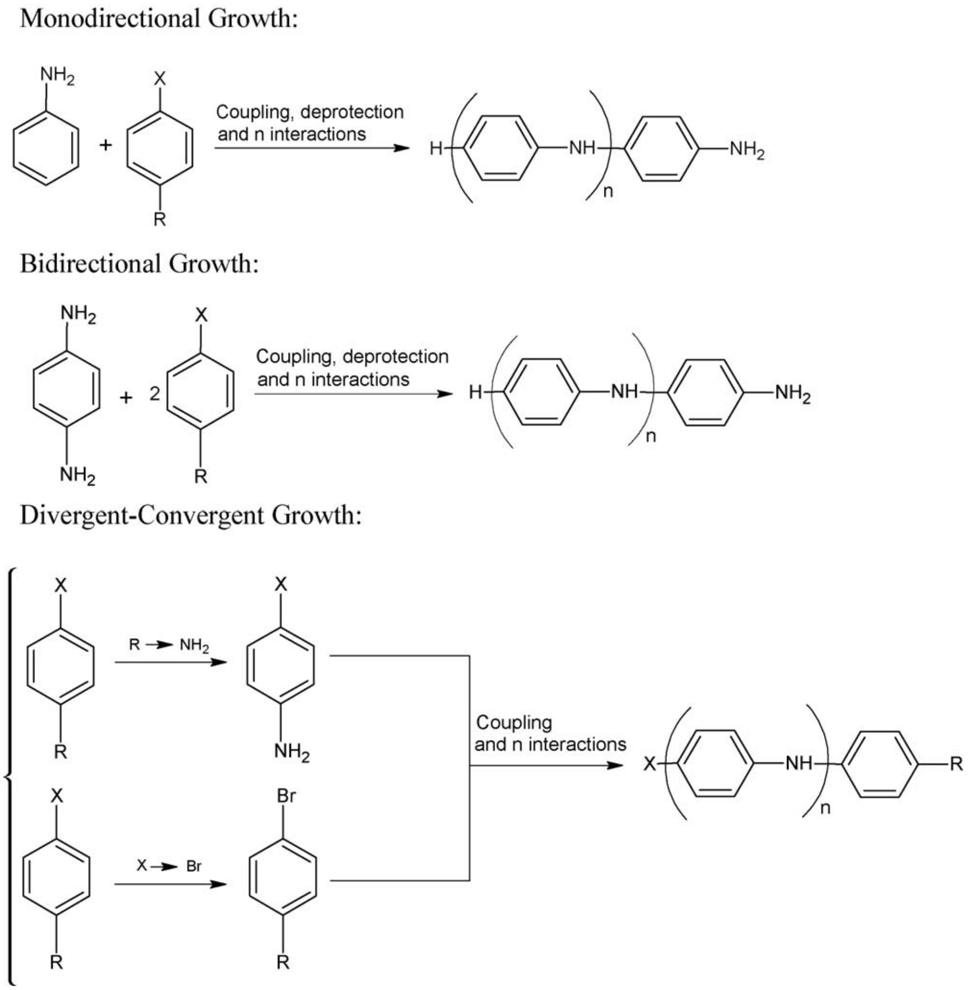

Scheme 17. Possible strategies for the synthesis of oligoanilines by aryl amination, X = Br, R = protector.

polymerization is completely suppressed with both the reagents. A strong catalytic effect is detected by using Cu, CuCl and $CuCl_2$, being all these simple copper compounds similarly efficient using either O_2 or H_2O_2 reagents, thus allowing yields up to 86–93% of emeraldine. The poisoning effect of acetonitrile is observed also in the case of the copper catalyzed reactions, but with a minor impact (5–14% decrement).

4.2. Pd-PANI

Differently from copper, palladium catalysis has been mainly developed as an aid for the growth of oligomeric chains starting from substituted monomers. The scientific background lies in the ability of palladium to catalyze the amination of aryl halide and triflate leading to a variety of arylamines [83]. In the 1998, Sadighi et al. reported on the palladium-catalyzed synthesis of monodisperse, controlled-length and functionalized oligoanilines taking advantage from the presence of a sacrificial orthogonal group to control the course of the reactions (see Scheme 17) [84]. The protective groups confer excellent solubility to the products and are easily removed to form the conductive oligomers.

A simple palladium-catalyzed synthesis of polyaniline involves the polymerization of 4-bromoaniline or the copolymerization of 1,4-phenylenediamine with 1,4-dibromobenzene.

Several strategies, illustrated in Scheme 17, may be envisioned for the synthesis of discrete oligoanilines by sequences of aryl amination and deprotection [85].

The reaction of an arylamine with a protected 4-bromoaniline, followed by deprotection, would result in an increase in the chain length of one unit for each iteration.

The disadvantages of such a method are the relatively slow increase in the chain length for a given number of steps and the growing difficulty in separating the products from any non-reacted starting material or by-products as the chain length increases. An outward growth of the oligoaniline from a symmetric core would permit the chain to grow up by two units in one interaction and result in a larger difference in size between starting material and desired product. As in the monodirectional strategy, the chain length increases by the same entity with each iteration of the sequence. A geometric increasing in the chain length is possible using a divergent-convergent approach [86]. In this strategy, a suitable protected oligomer is divided into two portions: one is converted to an arylamine and the other one to an aryl bromide. The coupling of the two products leads to a homologous oligomer, with a doubling in the chain length.

The facile electrophilic substitution of the trimethylsilyl group [87] allows it to function as a masked aryl bromide. However, a nitrogen protecting group is required to be stable under the reaction conditions of bromodesilylation, as well as under those of aryl amination, and to be removable without the use of strong acids, which would cleave the aryl-silicon bond. Among many different possibilities, it has been found that the diphenylmethylene group is particularly useful. Thus, the condensation of 4-bromoaniline with benzophenone is easily carried out on large scale and high

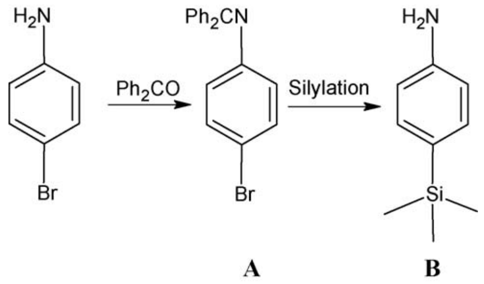

Scheme 18. Functionalization of arylamines.

yield. The resulting *N*-(diphenylmethylene)-4-bromoaniline (1) is a convenient substrate for palladium-catalyzed aryl amination, the reactions proceed rapidly and cleanly, with no detectable transamination, and the diphenylmethylene group imparts excellent crystal order to the products. This protective group is stable to bromine under the conditions used in bromodesilylation. The free primary amine may be liberated by hydrogenolysis [88] or by treatment with hydroxylamine under weakly acidic conditions [89].

Finally, the stability of the imine to alkyllithium reagents at low-temperature allows halogen-metal exchange to be carried out on *N*-(diphenylmethylene)-4-bromoaniline (1), leading to a convenient preparation of 4-(trimethylsilyl)aniline (2) (Scheme 18) [90].

Palladium-catalyzed coupling of *N*-(diphenylmethylene)-4-bromoaniline (1) and 4-(trimethylsilyl)aniline (2) affords an aniline dimer with a masked bromide at one end and a protected amine at the other one. Protection of the internal NH group as its *tert*-butyl carbamate (BOC) derivative forms a dimer derivative (3), which may be homologated by the divergent–convergent approach. The *tert*-butyl carbamate confers excellent solubility to intermediates and products, prevents the oxidation of the phenylenediamine moieties in higher oligomers to quinonediimines, and allows bromodesilylation to occur without detectable overbromination. The divergent-convergent process is easily carried out on multigram scale; the yield for each step is high, and the intermediates are easily purified by crystallization. Scheme 19 shows the synthesis of several chain fragments (5, 7, 10) used in the preparation of symmetric oligomers.

Other non-symmetric chain fragments may be prepared by modifications of this synthetic methodology.

Recently, Nadagouda and Varma reported that self-assembled Pd nanoparticles were able to catalyze the aniline polymerization to generate polyaniline nanocomposites [91].

4.3. Ag-PANI

Detailed studies have been recently devoted to the silver promoted oxidative polymerization of aniline, highlighting the role both of oxidant and activator of Ag^+ in photochemical oxidation.

The photopolymerization processes can be divided in two main categories:

1) Photopolymerization with photocatalytic systems.
2) Photoexcitation of the monomer leading to a conducting polymer [92].

According to the second point, de Barros et al. have described an innovative route to prepare polyaniline in which photons and metallic ions replace conventional oxidants to promote aniline polymerization [93].

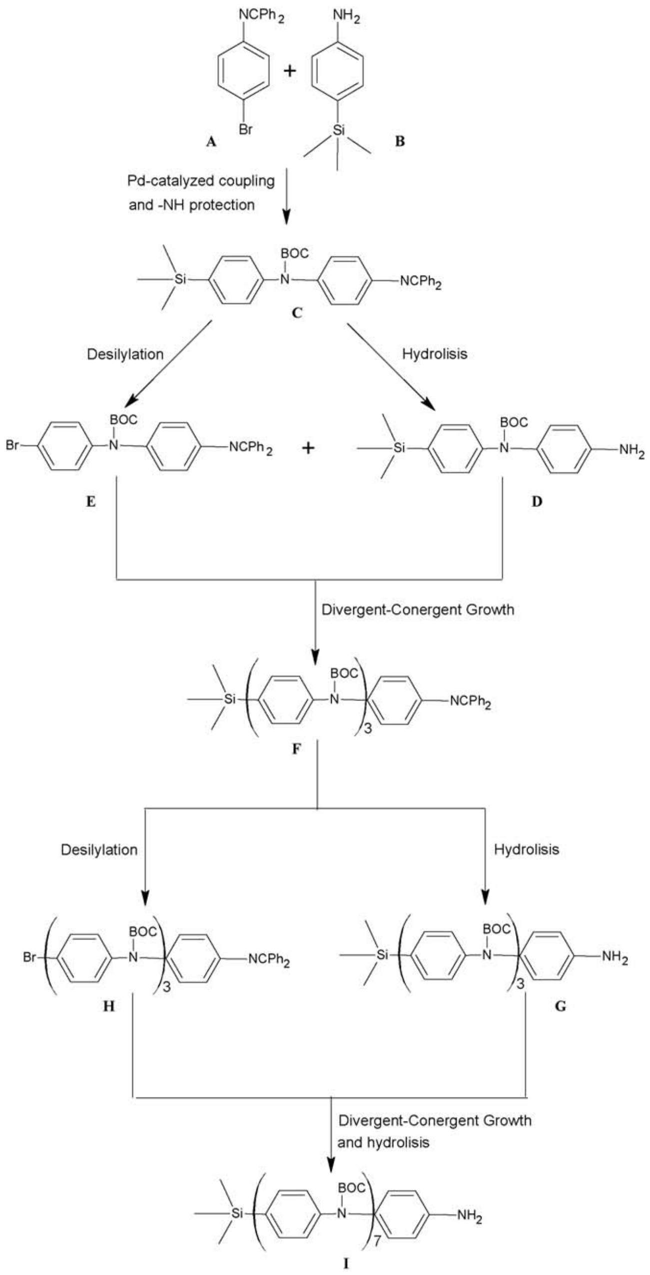

Scheme 19. Aniline oligomers preparation.

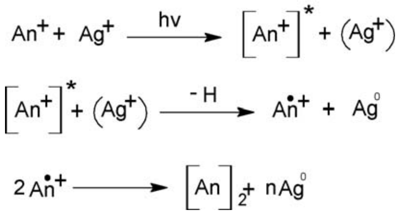

Scheme 20. Proposed mechanism for polyaniline composite synthesis.

Using photons in the UV or visible region to induce aniline polymerization in aqueous solution containing silver ions it has been observed a change of the colour from transparent to light green, reaching a steady state as a dark green solution. At the end of the process a green precipitate was obtained.

From the spectroscopic results the authors concluded that a mixture of emeraldine salt and emeraldine base was formed.

Scheme 20 shows the mechanism suggested to explain the polymer formation.

It has been observed that the polymerization does not occur in the dark. This implies that silver ions are unable to oxidize aniline monomer in aqueous solution. However, when a photon interacts with the solution, it promotes the aniline monomer to the excited state and then electrons can be transferred from the excited monomer to the silver ions leaving the aniline radical cation, which polymerizes through a head-to-tail coupling. The reductive process involves the reduction of silver cation to metal, thus promoting the formation of intriguing forms of metallic nanowires embedded in polyaniline.

The authors have observed that the polymerization dynamics is strongly dependent on the excitation energy. For the visible excitation, it has been observed that the time required for the polymerization is greater than that for UV excitation.

Similar results were reported by Khanna et al. during the reduction of silver nitrate to aniline by mild photolysis: following the absorption spectrum of the reactants, it has been shown that polyaniline formation takes place via *in situ* generation of small silver particles, ca 30 nm [94], while Nadagouda and Varma have reported, without any experimental details, that self-assembled Ag nanoparticles are able to catalyze the aniline polymerization [91].

4.4. Au-PANI

Incorporation of gold nanoparticles into polyaniline is a popular and interesting aspect of composite synthesis and a number of different methods have been suggested to produce exciting structures. The synthesis of gold–polyaniline composite materials was pioneered by Kang et al. [95]. They have recorded the spontaneous reduction and accumulation of elemental gold from chloroauric acid solution by electroactive polyaniline in the leucoemeraldine and emeraldine oxidation states. Eight years later, the same research group has published a more comprehensive work describing the synthesis of polyaniline, in the emeraldine form, and gold nanoparticle-composite produced in both *N*-methylpyrrolidinone and in aqueous medium [96]. Cattopadhyay and co-workers have reported on the preparation of gold–polyaniline composite material by using hydrogen peroxide, this latter acting as the oxidizing and the reducing agent [45]. This two-step process involves the reduction of $HAuCl_4$ to Au nanoparticles in aqueous medium followed by the oxidation of aniline resulting in the formation of a conducting composite. Many other methods have been reported for the preparation of Au-PANI composites [1,43,45,78,89–106], while the first paper reporting the use of colloidal gold as a catalyst for PANI preparation is more recent [74]. In the latter paper it has reported the oxidative polymerization of aniline using H_2O_2 as the oxidant and metallic gold as the catalyst. In the form of nanoparticles, gold produces the conductive polyaniline only in low yield. The short catalytic life of unsupported gold particles is assumed to be responsible for the limited aniline conversion to PANI. A great improvement of the oxidative polymerization of aniline has been obtained by using the more stable gold nanoparticles deposited on appropriate supporting materials, as carbon powder and titanium dioxide.

In particular, the high activity of 1%Au/TiO_2 has been ascribed to a strong contribution of the TiO_2 support. In fact, whereas unloaded carbon resulted to be inert in aniline polymerization by H_2O_2, titania, in form of a mixture of rutile and anatase (P25 TiO_2), promoted the partial oxidation to soluble dark oligomers which are precursors of polyaniline.

4.5. Fe-PANI

In 1991, Moon et al. have reported spectroscopic studies on the oxidation of polyaniline, in the reduced form of leucoemeraldine base, to the oxidized emeraldine base by using O_2 or H_2O_2 in the presence of $FeCl_3$-dibenzoyl peroxide catalytic system [107]. It has been found that, while the polymer solution is stable under inert atmosphere, the contact of the solution with air causes a colour change due to the oxidation by O_2. Although the role of oxygen in doping polyaniline has been already suggested [108], this experiment clearly shows its catalytic role in the leucoemeraldine oxidation.

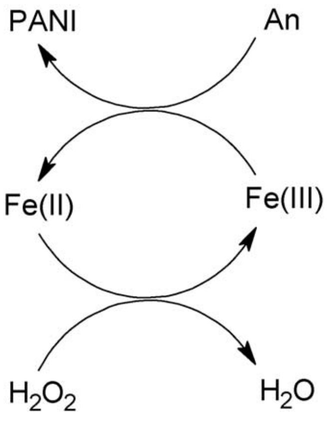

Scheme 21. Suggested mechanism of the polymerization of aniline iron(II)-catalyzed.

An interesting feature of the leucoemeraldine oxidation by O_2 is that the irradiation of light accelerates the oxidation process.

Leucoemeraldine undergoes oxidation also using H_2O_2, but only in the presence of catalytic amount of $FeCl_3$ under nitrogen atmosphere in the dark [109]. The reaction proceeds more rapidly than with oxygen. Moreover, the presence of $FeCl_3$ is indispensable to the oxidation in the dark, while the reaction with H_2O_2 under irradiation of the light proceeds slowly even in the absence of iron catalyst, probably due to photo-assisted decomposition of H_2O_2 to give radical species. Since the oxidation with H_2O_2 in the presence of Fe catalyst (Fenton reagent) is generally accepted to proceed through Fe-catalyzed decomposition of H_2O_2, thus giving [$\cdot$OH] radical which abstracts H from the substrate [110–114], the reaction reported by Moon is considered to involve abstraction of the N–H hydrogen of leucoemeraldine to give emeraldine.

Successively, Moon et al. have applied a similar catalytic system to aniline polymerization [71,80]. In fact, the use of H_2O_2–$FeSO_4$ system allows to produce polyaniline in high yields, up to 65%, under mild conditions. The prepared powdery emeraldine base is blue-black and shows high solubility in organic solvents. On the other hand, it shows similar chemical, physical and spectral properties as the previously prepared polyaniline using stoichiometric oxidants, as $(NH_4)_2S_2O_8$ [44,71].

Sun et al. have applied the same catalytic system, H_2O_2–$FeCl_2$–HCl, to the aniline polymerization, claiming improvements in the polymerization efficiency [44,80]. The proposed mechanism is reported in Scheme 21 [80].

The polyaniline derived by this method, however, exhibits low electrical conductivity owing to the presence of some branched structures.

Iron(III) is able to catalyze the aniline oxidation to emeraldine form by using ozone [115,116]. According to Yasuda and Shimidzu, iron(III) (0.77 V vs NHE) has a sufficient oxidation potential for the polymerization of aniline, while molecular oxygen (0.40 V vs NHE) has too low oxidation potential to convert iron(II) to iron(III). In contrast, ozone (2.1 V vs NHE) has enough high oxidation potential to convert either aniline to polyaniline or iron(II) to iron(III). The lack of reactivity in the absence of Fe(II) suggests the catalytic role of iron salts [115,117].

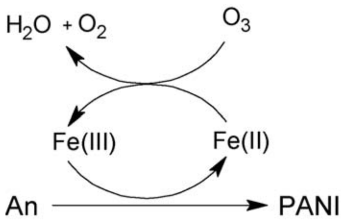

Scheme 22. Proposed catalytic cycles of the aniline polymerization by O3.

In such experiments, it has been observed that the yield and molecular weight are significantly influenced by the reaction temperature. The yield increases at higher temperature, similarly to the polymerization by ammonium peroxodisulfate [118]. On the other hand, also the molecular weight increases with the temperature, but this result is the opposite of the ammonium peroxodisulfate case [119]. The last result seems to indicate that the iron-assisted polymerization of aniline proceeds by a different mechanism from the case of ammonium peroxodisulfate. The electrical conductivities and the molecular weight of the iron-catalyzed polyaniline are much lower than those obtained by ammonium peroxodisulfate. Apparently, the lower molecular weight is considered responsible for the low electrical conductivity. In any case, the morphology of polyaniline powder could significantly influence the electrical conductivity of the resulting pellets according to the conduction mechanism of polyaniline [120]. In order to derive a correlation between molecular weight and electrical conductivity, a cast film from *m*-cresol solution of (±)-10-camphorsulfonic acid-doped polyaniline has been prepared [121]. The electrical conductivity of this film resulted to be similar to the one of the ammonium peroxodisulfate-derived PANI, thus underpinning that the molecular weight of PANI does not significantly influence the electrical conductivity of polyaniline. Interestingly, the low molecular weight of the polyaniline achieves a higher percentage of a soluble fraction of PANI suggesting new applications by solution-processing. Scheme 22 reports the condensed catalytic cycles for the aniline polymerization by O_3.

Conductive polymers which exhibit outstanding magnetic properties are of great interest in electronic applications [122–126]. In particular, Fe_3O_4 nanoparticles in combination to polyaniline have attracted attention because of their applications in colour imaging, magnetic recording media, soft magnetic materials and ferrofluids [127]. Developing innovative materials, many different morphologies of Fe_3O_4/PANI composites, such as core/shell spheres and 1 D structures have been developed [128–132].

In this context, Yang et al. have prepared PANI/Fe_3O_4 nanoparticle composites by polymerizing aniline with H_2O_2 in the presence of preformed Fe_3O_4 nanoparticles [133]. During this investigation, it has been demonstrated that carboxylic acids in the presence of specific buffers promote the formation of hydroxyl radical *via* H_2O_2 decomposition, thus favouring the polymerization of aniline. It has been already noted that a similar improvement of the reactivity can be obtained by using Fenton-like reagents [134,135] or horseradish peroxidise (HRP) [136–139]. However, while Fenton reagent takes effect by accelerating the decomposition of hydroxyl peroxide to hydroxyl radicals, the Fe^{3+} active centre of HRP catalyzes the oxidation of aromatic amines and phenols *via* the binding of H_2O_2 to generate organic free radicals derived from the substrate. Then, the resultant radicals undergo oxidative coupling and, after further oxidation and coupling reactions, the polymer is eventually formed [140].

Considering that Fe_3O_4 nanoparticles exhibit a peroxidase-like activity [141], Yang et al. have studied its use as a catalyst to prepare composite materials derived from aniline [133].

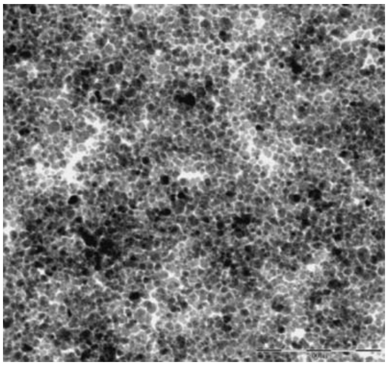

Fig. 11. TEM image of Fe_3O_4 nanoparticles (bar = 200 nm).

Owing to the interest in cleaner processes for the preparation of nanostructured magnetite-PANI materials, Rossi et al. have investigated the oxidative polymerization of *N*-(4-aminophenyl)-aniline using O_2 and H_2O_2 as the oxidants, in the presence of Fe_3O_4 nanoparticles. It has been found that, under appropriate conditions, ferrofluid magnetite [142] behaves as a catalyst for the oxidative polymerization of *N*-(4-aminophenyl)aniline leading to PANI-Fe_3O_4 composites in good yields. The unpublished results are here discussed in detail.

Ferrofluid magnetic nanoparticles were prepared according to a modified method derived from Xu et al. [143].

Thus, 6.0 g of $FeCl_3{\cdot}6H_2O$ and 2.2 g $FeCl_2{\cdot}4H_2O$ are dissolved in 25 mL of water and stirred under atmosphere of nitrogen at 80 °C. Then 12.5 mL of ammonia solution are added rapidly into the solution and the mixture is kept reacting for 30 min. To the black dispersion, 0.94 g of oleic acid are added and the stirring is continued for 90 min.

The magnetic powder is collected by a magnet at the bottom of the beaker, the surnatant liquid removed and the solid residue washed several times with water.

After drying overnight in the air, the solid material (3.0 g) is transferred into toluene (10 mL) resulting in a stable magnetic “ferrofluid colloid”. According to ICP analysis, the content of magnetite in toluene resulted to be 40% (w/w), while from TEM image (Fig. 11) and XRD analysis (Fig. 12) the mean diameter of magnetic nanoparticles was 11 nm.

PANI/Fe_3O_4 composites have been prepared starting from aniline dimer and using either O_2 or H_2O_2 as the oxidants. In the first case, aniline dimer (460 mg, 2.5 mmol) and the desired amount of colloidal sol were dissolved in 5 mL of toluene. Then water (15 mL) and aqueous 1 M HCl (2.5 mL) were added and the dispersion stirred under oxygen at 3 bar for 3 days.

The resulting dark solid was collected by filtration washed with acetone, in order to remove soluble oligomers, and dried at 383 K overnight. A blank test, carried out in the same condition but in the absence of magnetite, showed no conversion after 3 days.

In the oxidation with hydrogen peroxide, the reaction was carried out in a similar manner, by adding an excess of H_2O_2

Table 1
Polymerization of N-(4-aminophenyl)aniline by O_2 (3 bar) in the absence and in the presence of Fe_3O_4.

Experiment	AD/Fe_3O_4 (molar ratio)	Yield%
1	No magnetite	0
2	681	9
3	342.5	10
4	228	14
5	137	25
6	50	46
7	20	55

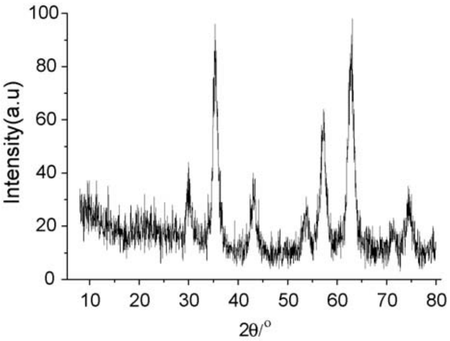

Fig. 12. X-ray diffraction pattern of Fe_3O_4 nanoparticles.

(H_2O_2/AD = 3 molar ratio) to the other reagents. The resulting mixture was stirred at room temperature for 24 h.

The results show that using dioxygen a clear catalytic effect is detected, because the yield of the collected product grows up from zero to 55% by increasing the Fe_3O_4 amount up to AD/Fe_3O_4 = 20 (Table 1, exp. 7).

Using H_2O_2, the catalytic effect is less clear because the polymerization took place also in the absence of any catalyst producing the polymeric material in 43% yield after 24 h. On adding colloidal Fe_3O_4, the yield increased to 67% at AD/Fe_3O_4 = 20 (Table 2, exp. 14).

All the polymeric materials contain emeraldine salt, as it resulted from FT-IR, UV–vis and XRD analysis. Concerning the morphological aspects, TEM and SEM images (Fig. 13) show a nanorod-like structure of 29–107 nm size for the polymeric material. The Electron Spectroscopic Imaging (ESI) analysis shows that Fe_3O_4 nanoparticles in the polymeric matrix are not uniformly dispersed.

The magnetic properties of the composites have been investigated by means of the characteristic plots of magnetization vs an applied magnetic field at 300 K, reported in Fig. 14.

The lack of hysteresis agrees with the superparamagnetic behaviour, as observed in previous systems containing Fe_3O_4 NPs [144–147]. In particular, reversible magnetization curves with zero coercive field are expected at room temperature for Fe_3O_4 nanoparticles with diameters lower than 20 nm. Also the shape of the magnetization curves, reaching the saturation magnetization (M_s) above 3 kOe, fits the literature data. These findings indicate that magnetite nanoparticles maintain their magnetic properties in the PANI-Fe_3O_4 composites.

The conductivity, correlated to the bulk resistance of the present PANI/Fe_3O_4 material, is similar to that obtained in the conventional chemical polymerization using stoichiometric reagents (10^{-2} to 10^{-3} S cm^{-1}, Table 3) [148,149].

Table 2
Catalytic oxidative polymerization of AD by H_2O_2 in the absence and in the presence of Fe_3O_4.

Experiment	AD/Fe_3O_4 (molar ratio)	H_2O_2/AD (molar ratio)	Yield%
8	No magnetite	3	40
9	3000	3	40
10	1000	3	41
11	681	3	55
12	342	3	54
13	50	3	62
14	20	3	67

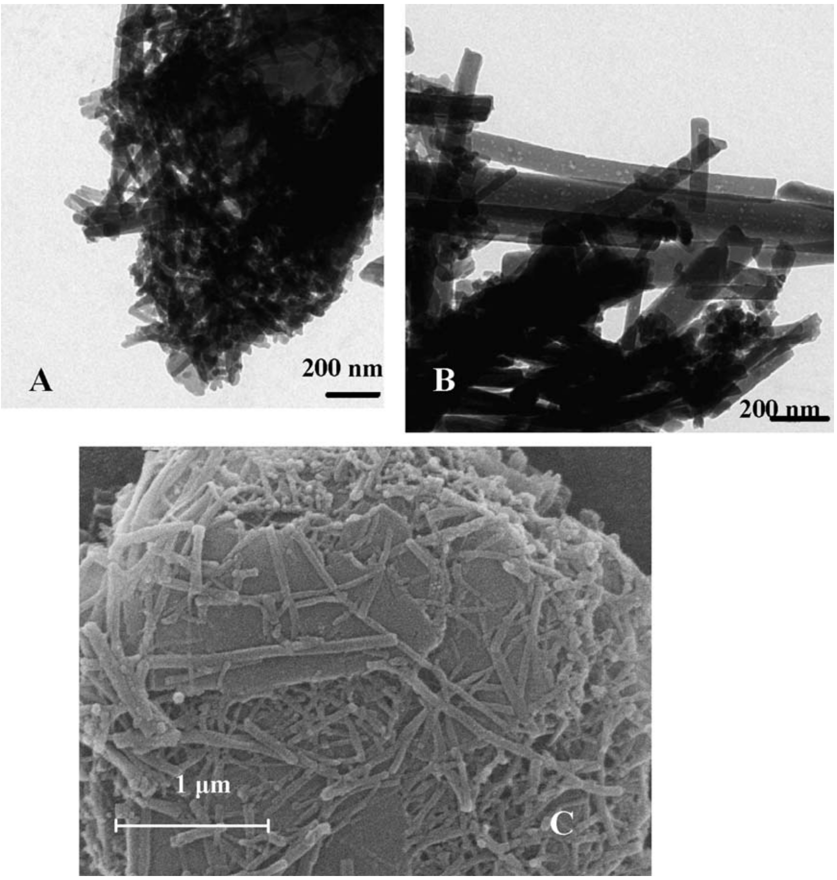

Fig. 13. TEM (A and B, bar = 200 nm) and SEM (C, bar = 1 µm) images of Fe_3O_4/polyaniline composites.

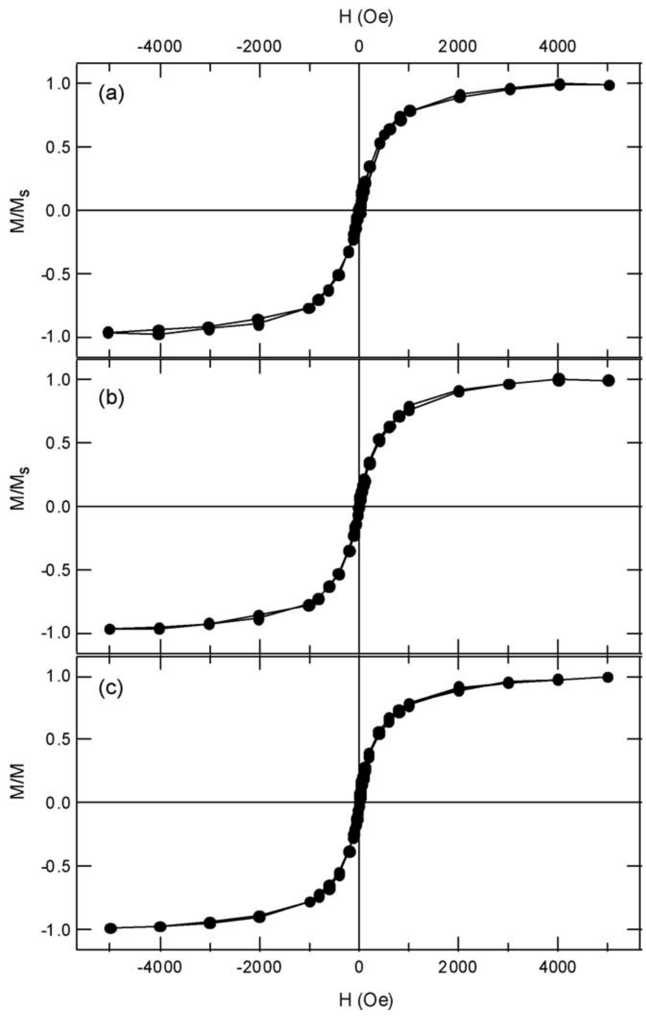

Fig. 14. Magnetization curves at 300 K for PANI-Fe_3O_4 composites (a = exp. 14, b = exp. 7, c = exp.13).

It should be pointed out that the effect of pressure, pressing time and interval between pressing and testing, which can modify the interchain and intrachain conductivity of the polymers, were not evaluated [150]. The whole experiments indicate that Fe_3O_4 nanoparticles present a strong catalytic activity in the aerobic polymerization of *N*-(4-aminophenyl)-aniline and a lower effect in the case of H_2O_2, without the need of using soluble co-catalysts. No particular templating effects seem to be due to the presence of Fe_3O_4. Zhang et al., however, reported on composite nanostructures of PANI containing magnetic nanoparticles (e.g. Fe_3O_4 or Fe_2O_3) prepared by *in situ* doping polymerization in the presence of H_3PO_4 as the dopant and $(NH_4)_2S_2O_8$ as the oxidant. It has been proposed that the micelles containing Fe_3O_4 act as the soft templates to co-structure PANI-H_3PO_4/Fe_3O_4 composite nanotubes or nanofibres *via* a self-assembly process, while nanoneedle-like Fe_2O_3 plays a hard template role to form coaxial PANI-H_3PO_4-Fe_2O_3 nanoneedles. The resulting composite nanostructures showed electrical and magnetic properties that could be adjusted by changing the structure and content of the used magnetic nanoparticles [151].

Table 3
Conductivity data of PANI and PANI-Fe_3O_4 composites.

Sample	0 V (S cm^{-1})	0.5 V (S cm^{-1})	1 V (S cm^{-1})
7	1.6×10^{-2}	1.6×10^{-2}	1.6×10^{-2}
8	2.7×10^{-2}	3.4×10^{-2}	7.9×10^{-2}
13	4.1×10^{-3}	8.1×10^{-3}	2.8×10^{-2}
14	2.0×10^{-2}	2.5×10^{-2}	5.4×10^{-2}

4.6. Polypyrrole

The metal-assisted polymerization of pyrrole and substituted pyrroles has attracted less attention with respect to aniline polymerization. However, the present interest in clean processes for producing polypyrroles is proven by new emerging synthetic strategies and novel exciting applications.

4.6.1. Cu-PPY

The Cu-catalyzed polymerization of pyrrole by using the $AlCl_3$-CuCl-O_2 catalytic system has been reported in 1990 by Toshima and Tayanagi [150]. When *p*-xylene, nitromethane and nitrobenzene were used as the solvents, the yield of polymer resulted to be very high but the elemental analysis was far from the calculated value for PPY (C_4H_3N) and the conductivity was quite low (10^{-10} S cm^{-1}). On the contrary, in acetonitrile the polymeric product showed elemental analysis close to the expected value and the conductivity increased by several orders up to 10^{-2} S cm^{-1}. However, even in the case of acetonitrile, the product showed contamination from Cl and O which was ascribed to chlorine, carbonyl and hydroxyl groups bound to the polymeric backbone.

Dias et al. have investigated catalytic methods for the large scale synthesis of polypyrrole in aqueous media using three different catalysts, Fe^{3+}, Ce^{4+} and Cu^{2+} and hydrogen peroxide as the oxidant [152]. The best results were obtained using Fe^{3+} (up to 90%), while with Ce^{4+} and Cu^{2+} the yield was very low (<18% and ~4% respectively).

The reaction carried out under identical conditions, but in the absence of any catalyst, did not give any precipitate but only a dark solution indicating a slow polymerization process [153]. Considering also the standard electrode potentials, it has been demonstrated in a pure thermodynamic perspective hydrogen peroxide is capable of polymerizing pyrrole, but it undergoes kinetic limitations. Therefore, the role of hydrogen peroxide is to regenerate the oxidized form of the metal ion which acts as the oxidant towards the organic substrate. In the case of Cu^{2+}, which presents a low, insufficient potential, it is assumed its catalytic role in the decomposition of hydrogen peroxide thus decreasing the activation energy for the oxidative polymerization of pyrrole [154].

4.6.2. Pd-PPY

Literature reports very few papers about the Pd-catalyzed polymerization of pyrrole. Nadagouda and Varma have observed that self-assembled Pd nanoparticles are able to catalyze the polymerization of pyrrole to the corresponding metal–polymer nanocomposites [91].

During this research it has been observed that Pd-catalyzed polypyrrole yielded a material in form of quite interesting one-dimensional nanofibers, in contrast to other synthetic methods leading to more conventional spherical composites [155].

4.6.3. Au-PPY

In 2009 Rossi and co-workers have reported, for the first time, the facile polymerization of pyrrole using O_2 and H_2O_2 as the oxidants in aqueous solution under mild conditions catalyzed by colloidal gold [73].

Stirring the aqueous solution of pyrrole hydrochloride at room temperature for several days, under air in the absence of gold nanoparticles, no insoluble product was collected from the dark solution, meaning that only low molecular weight polymers were formed in the spontaneous autoxidation. On the contrary, by adding colloidal gold to the reactants, a dark polymeric material, insoluble in acetone, was smoothly achieved while the yield increased, up to

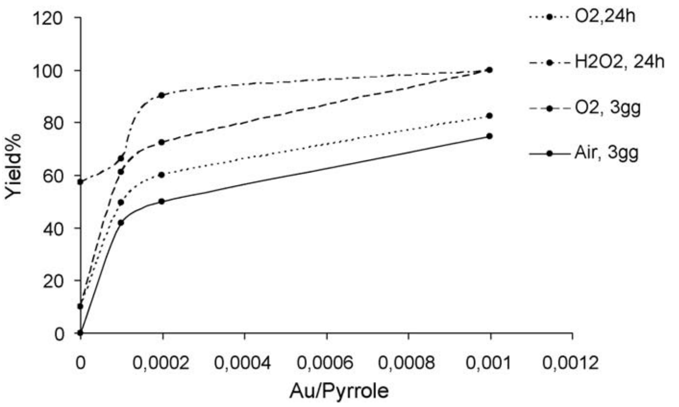

Fig. 15. Gold effect in the polymerization of pyrrole by air, O_2 and H_2O_2.

75%, by growing up gold concentration (in any case, less than 0.1% with respect to the reacting monomer).

Using pure dioxygen under pressure (3 bar), a slow auto-oxidation produced a modest yield of insoluble polymer (12%) after 3 days. On adding colloidal gold, a strong catalytic effect was detected: the polymeric material was obtained with almost total yield (99%) in 3 days.

With hydrogen peroxide as the oxidant, a consistent polymerization of pyrrole was observed already in the absence of catalyst, producing 57% of the polymeric material in 24 h.

Note that this result is in contrast with previous reported data concerning the non-catalyzed oxidation of pyrrole by H_2O_2 [152,153].

However, also in this case, a catalytic contribute of gold is demonstrated by the increment of the yield, up to 99%, on addition of a small quantity of colloidal metal (Py/Au = 1000).

Fig. 15 shows the catalytic effect of gold in PPy formation with different reagents.

The kinetics of polypyrrole formation by dioxygen in the presence of different quantities of gold is illustrated in Fig. 16.

Concerning morphological aspects, different structures have been observed according to different experimental procedure. By using H_2O_2, the quick polymerization led to a partly reticulated structure in the absence of gold, and to amorphous material using gold catalysis. The low-yield, non-catalyzed polymerization with gaseous oxygen produced more ordered structures represented by 40–80 nm spheres, whereas a large amount of curious thin squares (20–60 nm) were observed in the high yield polymerization catalyzed by gold (Fig. 17).

This latter structure is unusual also in the context of conventional polymerizations of pyrrole and could be of interest for tailor-made composite applications.

The conductivity correlated to the bulk resistance of the synthesized polypyrrole materials, 2.7×10^{-4} to 5×10^{-3} S cm^{-1}, is similar to that obtained in conventional chemical polymerization using stoichiometric reagents [156], but much lower than the values generally found in electrochemical film deposition [157].

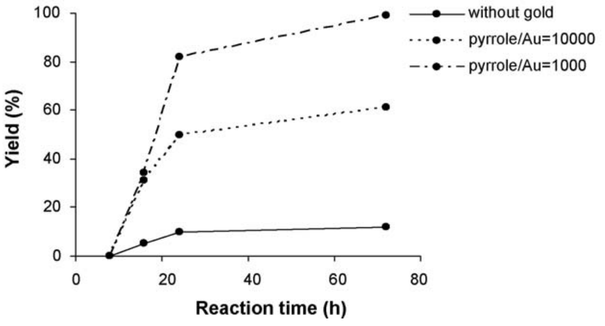

Fig. 16. Kinetic data of pyrrole polymerization under O_2.

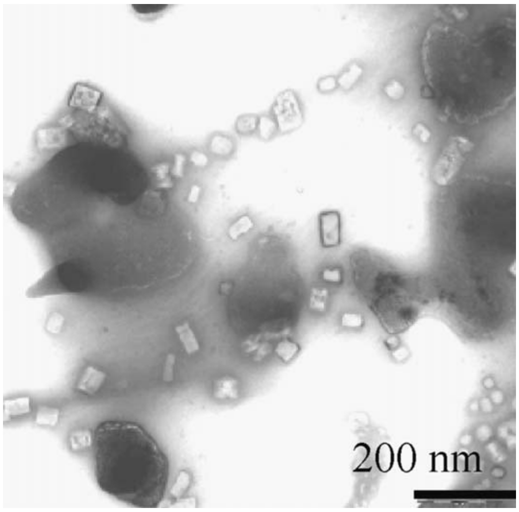

Fig. 17. TEM images of polypyrrole sample obtained by O_2, Py/Au = 5000.

4.6.4. Fe-PPY

A drawback in using iron trichloride as oxidant for pyrrole polymerization is that at least two moles of reagent per mole of pyrrole are needed and hydrogen chloride is formed as the by-product [158]. The development of an effective method for a large production of polypyrrole by means of cheap iron catalyst would be a great advantage, either from an ecologic point of view or economic reasons [67,159]. In 1996, Toshima and Ihata observed that homogeneous catalysis could occur under molecular oxygen but in the presence of relatively high amount of iron(III) salts (1:10 molar ratio with respect to the reacting monomer) [159]. Under the polymerization conditions, the couple Fe(II)-Fe(III) acts as the oxygen transfer thus ensuring a catalytic effect. According to different solvents (water, ethanol, 2-butanone, acetonitrile, nitromethane, propylene carbonate) the yield and the structure of the formed polymer changed and propylene carbonate has been found to be best choice. Starting from Fe(II) salts, the kinetics of polymerization is slower and the conductivity of the resulting material lower. An improvement to the Fe(II) catalysis can be inferred by the use of specific electrolytes as tetrabutylammonium salts. Although during the pyrrole polymerization both oxygen consumption and yield decrease with addition of the ammonium salt, the conductivity of the product is improved by about one order of magnitude, in particular using tetrabutylammonium bromide.

As an interpretation of the improved conductivity, it has been supposed that the anion works as a dopant showing the best properties increasing with its size (Stock radius).

The authors have suggested two possible mechanisms for the iron-catalyzed polymerization: (1) catalytic oxidative polymerization *via* complex formation, and (2) catalytic oxidative polymerization without the intermediate complex. The reaction schemes for both mechanisms are reported below:

1) Catalytic oxidative polymerization via complex formation:

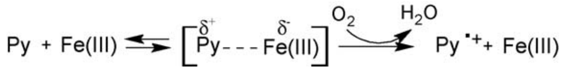

2) Catalytic oxidative polymerization without complex formation:

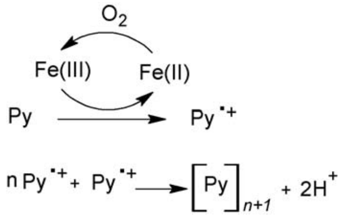

In the mechanism 1, iron(III) chloride assists the oxidation of pyrrole with molecular oxygen by forming the complex $Py^{\delta+}$-$FeCl_3^{\delta-}$.

In mechanism 2, pyrrole is oxidized by iron(III), and the produced iron(II) is oxidized by molecular oxygen. In this latter case, the solvent effect can be explained by the fact that the redox potential of the iron(III) complex depends on the solvent. Thus, the iron(III) complex has a higher potential in propylene carbonate than in acetonitrile or ethanol. In other words, iron(III) ion coordinated by propylene carbonate has stronger oxidation ability than that in acetonitrile or ethanol.

A soluble conductive polymer was obtained from 3-butoxycarbonyl-4-methylpyrrole in presence of iron(III) as a catalyst by Ohno and Toshima [160]. Although the authors have observed that the addition of $BF_3 \cdot Et_2O$ to the reaction system can increase the yield of the polymer, the role of the promoter has not been elucidated.

Also in this case, the proposed reaction mechanism (Scheme 23) invokes the role of the Fe(II)-Fe(III) couple:

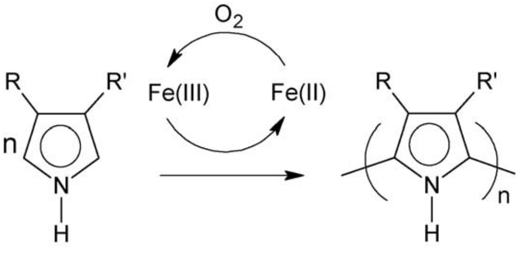

Scheme 23. Reaction scheme of the catalytic polymerization of 3-butoxycarbonyl-4-methylpyrrole by iron catalysis ($R = CH_3$, $R' = COOBu$).

5. Applications

Conductive polymers are attractive for new product concepts and for replacing conventional materials due to their unique combination of easy processing, stability, controllable conductivity, optical and mechanical properties. Many different industrial fields take advantage from the applications of polyaniline and polypyrrole conductors:

1) *Packaging industry*: Injection moulded antistatic products, antistatic films.
2) *Electronic field*: Antistatic packaging of components, printed circuit boards.
3) *Fenestration*: Electrochromic “smart” windows, electrochromic automobile rear vision systems.
4) *Textile industry*: Conductive fabrics.
5) *Automotive industry*: Antistatic charge dissipation, paint primers, electrochromic rear vision systems.
6) *Construction*: Antistatic floors, antistatic work surfaces.
7) *Mining*: Conductive pipes for explosives, antistatic packaging.

New interesting perspectives are involving conductive nanometric devices as nanotubes and nanofibers for biological uses [161,162], or nanostructured electrodes for fuel cells [163,164].

In conclusion, after forty years of studies on conducting polyaniline and polypyrrole, many basic problems related to synthetic methods and reaction mechanism are still actual, being the investigations of the polymerization of aniline intercalated into montmorillonite clay an exhaustive example [165].On the other hand, the continuous interest in the preparation and characterization of metal composites, as gold-PANI nanostructured materials [166], produces new exciting applications as those concerning the analytical detection of biological target molecules [167].

Acknowledgements

We thank Dr. Zhi Chen for the experimental work carried out during his post-doc stage at the University of Milano.

References

[1] K. Mallick, M.J. Witcomb, A. Dinsmore, M.S. Scurrell, Macromol. Rapid Commun. 26 (2005) 232.
[2] K. Mallick, M.J. Witcomb, A. Dinsmore, M.S. Scurrell, J. Polym. Res. 13 (2006) 397.
[3] X. Lu, D. Chao, J. Chen, W. Zhang, Y. Wei, Mater. Lett. 60 (2006) 2851.
[4] H. Yoneyama, K. Wakamoto, H.J. Tamuré, J. Electrochem. Soc. 132 (1985) 2414.
[5] K. Kaneto, M. Maxfield, D.P. Nairns, A.G. MacDiarmid, A.J. Heeger, J. Chem. Soc. Faraday Trans. 78 (1982) 3417.
[6] J.W. Thackeray, H.S. White, M.S. Wrighton, J. Phys. Chem. 89 (1985) 5133.
[7] S. Kuwabata, S. Ito, H. Yoneyama, J. Electrochem. Sci. Technol. 135 (1998) 1691.
[8] P.N. Bartlett, S.K. Ling Chung, Sens. Actuators 20 (1989) 287.
[9] D.T. Hao, T.N. Suresh Kumar, R.S. Srinivasa, R. Lal, N.S. Punekar, A.Q. Contractor, Anal. Chem. 64 (1992) 2645.
[10] I. Sapurina, A. Riede, J. Strejskal, Synth. Met. 123 (2001) 503.
[11] X. Feng, C. Mao, G. Yang, W. Hou, J. Zhu, Langmuir 22 (2006) 4384.
[12] A.J. Epstein, J.M. Ginder, F. Zuo, R.W. Bigelow, H.S. Woo, D.B. Tanner, A.F. Richter, W.S. Huang, A.G. MacDiarmid, Synth. Met. 18 (1987) 303.
[13] P. Snauwaert, R. Lazzaroni, J. Riga, J.J. Verbist, J. Chem. Phys. 92 (1990) 2187.
[14] N.V. Blinova, J. Stejskal, M. Trchová, J. Prokes, Polymer 47 (2006) 42.
[15] J. Stejskal, R.G. Gilbert, Pure Appl. Chem. 74 (2002) 857.
[16] N.V. Blinova, J. Strejskal, M. Trchová, J. Prokes, M. Omastová, Eur. Polym. J. 43 (2007) 2331.
[17] D.C. Trivedi, Polyanilines, in: H.S. Nalwa (Ed.), Handbook of Organic Conductive Molecules and Polymers, vol. 2, Wiley, 1997, p. 505.
[18] S.R. Elliot, The Physics and Chemistry of Solids, John Wiley and Sons, 1998.
[19] Defence R&D Canada-Atlantic (DRDC Atlantic) TM 2003-005.
[20] S. Sadki, P. Schottland, N. Brodie, G. Sabouraud, Chem. Soc. Rev. 29 (2000) 283.
[21] P. Xu, X.J. Han, C. Wang, B. Zhang, H.L. Wang, Synth. Met. (2009) 430.
[22] K. Doblhofer, K. Rajeshwar, in: T.A. Skotheim, R.L. Elsenbaumer, J.R. Reynolds (Eds.), Handbook of Conducting Polymers, 2nd ed., Marcel Dekker, 1998, p. 531.
[23] A.J. Bard, L.R. Faulkner, Electrochemical Methods, Fundamentals and Applications, John Wiley & Sons, New York, 1980.
[24] J. Rodriguez, H.J. Grande, T.F. Otero, in: H.S. Nalwa (Ed.), Handbook of Organic Conductive Molecules and Polymers, John Wiley & Sons, 1997, p. 415.
[25] M.E.G. Lyons, Advances in chemical physics, Polym. Syst. 94 (1997) 297.
[26] B.L. Funt, A.F. Diaz, Organic Electrochemistry: an Introduction and a Guide, Marcel Dekker, 1991, p. 1337.
[27] E.M. Genies, G. Bidan, A.F. Diaz, J. Electroanal. Chem. 149 (1983) 101.
[28] R.J. Waltman, J. Bargon, Can. J. Chem. 64 (1985) 76.
[29] R.J. Waltman, J. Bargon, Tetrahedron 40 (1984) 3963.
[30] P. Pfluger, M. Krounbi, G.B. Street, J. Chem. Phys. 78 (1983) 3212.
[31] G.B. Street, in: T.J. Skotheim (Ed.), Handbook of Conducting Polymers, 1st ed., Marcel Dekker, New York, 1986, p. 188.
[32] P. Pfluger, G.B. Street, J. Chem. Phys. 80 (1984) 544.
[33] K.J. Kim, H.S. Song, J.D. Kim, Bull. Korean Chem. Soc. 9 (1988) 248.
[34] Y.T. Kim, R.W. Collins, K. Vedom, D.L. Allara, J. Electrochem. Soc. 138 (1991) 3266.
[35] S. Asavapiriyanont, G.K. Chandler, G.A. Gunawardena, D. Pletcher, J. Electroanal. Chem. 177 (1984) 229.
[36] Q. Pei, R. Qian, Synth. Met. 45 (1991) 35.
[37] M. Satoh, K. Imanishi, K. Yoshino, J. Electroanal. Chem. 317 (1991) 139.
[38] C.A. Salzer, C.M. Elliott, S.M. Hendrickson, Anal. Chem. 71 (1999) 3677.
[39] M. Takakubo, J. Electroanal. Chem. 258 (1989) 303.
[40] Y.J. Qiu, J.R. Reynolds, J. Polym. Sci. A 30 (1992) 1315.
[41] A. Boyle, J.P. Penneau, E. Genies, C. Riekiel, J. Polym. Sci. B 30 (1992) 265.
[42] K. Mallick, M.J. Witcomb, A. Dinsmore, M.S. Scurrell, Langmuir 21 (2005) 7964.
[43] Y. Wang, Z. Liu, B. Han, Z. Sun, Y. Huang, G. Yang, Langmuir 21 (2005) 833.
[44] Z. Sun, Y. Geng, J. Li, X. Wang, X. Jing, F. Wang, J. Appl. Polym. Sci. 72 (1999) 1077.
[45] T.K. Sarma, D. Chowdhury, A. Paul, A. Chattopadhyay, Chem. Commun. (2002) 1048.

[46] Y. Wei, G.-W. Jang, Ch.-Ch. Chan, K.F. Hsuen, R. Hariharan, S.A. Patel, C.K. Whitecar, J. Phys. Chem. 94 (1990) 7716.
[47] Y. Wei, X. Tang, Y. Sun, W.W. Focke, J. Polym. Sci. 27 (1989) 2385.
[48] Y. Wei, R. Hariharan, S.A. Patel, Macromolecules 23 (1990) 758.
[49] Y. Wei, K.F. Hsueh, G.W. Jang, Polymer 35 (1994) 3572.
[50] E.M. Genie, M.J. Lapkowski, Electroanal. Chem. 236 (1987) 199.
[51] N. Gospodinova, P. Mokreva, L. Terlemezyan, Polymer 34 (1993) 1330.
[52] N. Gospodinova, L. Terlemezyan, P. Mokreva, K. Kossev, Polymer 34 (1993) 2434.
[53] N. Gospodinova, P. Mokreva, L. Terlemezyan, Polymer 34 (1993) 2438.
[54] N. Gospodinova, L. Terlemezyan, P. Mokreva, A. Tadjer, Polymer 37 (1996) 4431.
[55] N. Gospodinova, P. Mokreva, L. Terlemezyan, Polymer 36 (1995) 3585.
[56] N. Gospodinova, P. Mokreva, L. Terlemezyan, Polymer 35 (1994) 3102.
[57] N. Gospodinova, P. Mokreva, L. Terlemezyan, Polym. Int. 41 (1996) 79.
[58] N. Gospodinova, P. Mokreva, L. Terlemezyan, Chem. Commun. (1992) 923.
[59] J. Stejskal, P. Kratochvil, N. Gospodinova, L. Terlemezyan, P. Mokreva, Polymer 33 (1992) 4857.
[60] N. Gospodinova, L. Terlemezyan, P. Mokreva, J. Stejskal, P. Kratochvil, Eur. Polym. J. 29 (1993) 1305.
[61] E. Sreitwieser, Teoria moleculiarnih orbit, Moscow, 1995.
[62] A.G. MacDiarmid, A.J. Epstein, Synth. Met. 69 (1995) 85.
[63] R.L. Elsembaumer, C.C. Han, K.Y. Jen, US Pat. 5-160-457 (1992).
[64] S. Trakhtenberg, Y. Hangun-Balkir, J.C. Warner, F.F. Bruno, J. Kumar, R. Nagarajan, L.A. Samuelson, J. Am. Chem. Soc. 127 (2005) 9100.
[65] W. Liu, A. Anagnostopoulos, F.F. Bruno, K. Senekal, J. Kumar, S. Tripathy, L. Samuelson, Synth. Met. 101 (1999) 738.
[66] N. Bicak, B. Karagoz, J. Polym. Sci. A 44 (2006) 6025.
[67] N. Toshima, S. Hara, Prog. Polym. Sci. 20 (1995) 155.
[68] S.E. Bourdo, B.C. Berry, T. Viswanathan, J. Appl. Polym. Sci. 98 (2005) 29.
[69] W. Liu, A.L. Cholli, R. Nagarajan, J. Kumar, S. Tripathy, F.F. Bruno, L. Samuelson, J. Am. Chem. Soc. 121 (1999) 11345.
[70] W. Liu, J. Kumar, S. Tripathym, J. Senecal, L. Samuelson, J. Am. Chem. Soc. 121 (1999) 71.
[71] D.K. Moon, K. Osokada, T. Maruyama, T. Yamamoto, Makromol. Chem. 193 (1992) 1723.
[72] Z. Chen, C. Della Pina, E. Falletta, M. Rossi, J. Catal. 267 (2009) 93.
[73] C. Della Pina, E. Falletta, M. Lo Faro, M. Pasta, M. Rossi, Gold Bull. 42 (2009) 27.
[74] Z. Chen, C. Della Pina, E. Falletta, M. Lo Faro, M. Pasta, M. Rossi, N. Santo, J. Catal. 259 (2008) 1.
[75] N. Bicak, B. Karagoz, J. Polym. Chem. 44 (2006) 6025.
[76] H.V.R. Dias, R.M.G. Rajapakse, D.M.M. Krishantha, M. Fianchini, X. Wang, R.L. Elsenbaumer, J. Mater. Chem. 17 (2007) 1762.
[77] H.V.R. Dias, X. Wang, R.M.G. Rajapakse, R.L. Elsenbaumer, Chem. Commun. (2006) 976.
[78] M. Sivakumar, A. Gedanken, Synth. Met. 148 (2005) 301.
[79] Y. Wang, X. Jing, J. Kong, Synth. Met. 157 (2007) 269.
[80] Z. Sun, Y. Geng, J. Li, X. Jing, F. Wang, Synth. Met. 84 (1997) 99.
[81] Z. Jin, Y. Su, Y. Duan, Synth. Met. 122 (2001) 237.
[82] N. Toshima, H. Yan, M. Ishiwatari, Bull. Chem. Soc. Jpn. 67 (1994) 1947.
[83] J.P. Wolfe, J. Åhman, J.P. Sadighi, R.A. Singer, S.L. Buchwald, Tetrahedron Lett. 38 (1997) 6367.
[84] J.P. Sadighi, R.A. Singer, S.L. Buchwald, J. Am. Chem. Soc. 120 (1998) 4960.
[85] J.M. Tour, Chem. Rev. 96 (1996) 537.
[86] E. Igner, O.I. Paynter, D.J. Simmonds, M.C. Whiting, J. Chem. Soc., Perkin Trans. I (1987) 2447.
[87] B. Bennetau, J. Dunogues, Synlett (1993) 171.
[88] L. Wessjohann, G. McGaffin, A. de Meijere, Synthesis (1989) 359.
[89] K.J. Fasth, G. Antoni, B. Langström, J. Chem. Soc., Perkin Trans. I (1988) 3081.
[90] D.M.R. Walton, J. Chem. Soc. C (1966) 1706.
[91] M.N. Nadagouda, R.S. Varma, J. Nanomater. (2008) 1.
[92] N. Kobayashi, K. Teshima, R. Hirohashi, J. Mater. Chem. 8 (1998) 497.
[93] R.A. de Barros, W.M. de Azevedo, F.M. de Aguiar, Mater. Charact. 50 (2005) 131.
[94] P.K. Khanna, N. Singh, S. Charan, A.K. Viswanath, Mater. Chem. Phys. 92 (2005) 214.
[95] E.T. Kang, Y.P. Ting, K.G. Neoh, K.L. Tan, Polymer 34 (1993) 4994.
[96] J. Wang, K.G. Neoh, E.T. Kang, J. Colloid Interface Sci. 239 (2001) 78.
[97] K. Mallick, M.J. Witcomb, M.S. Scurrell, Gold Bull. 39 (2006) 166.
[98] Z. Wang, J. Yuan, D. Han, L. Niu, A. Ivaska, Nanotechniques 18 (2007) 115610.
[99] S.K. Pillalamarri, F.D. Blum, M.F. Bertino, Chem. Commun. (2005) 4584.
[100] J.A. Smith, M. Josowicz, M. Engelhard, D.R. Baer, J. Janata, Phys. Chem. Phys. 7 (2005) 3619.
[101] K. Mallick, M.J. Witcomb, M.S. Scurrell, J. Mater. Sci. 41 (2006) 6189.
[102] K. Huang, Y. Zhang, Y. Long, J. Yuan, D. Han, Z. Wang, L. Niu, Z. Chen, Chem. Eur. J. 12 (2006) 5314.
[103] K. Mallick, M.J. Witcomb, M.S. Scurrell, A.M. Strydom, Gold Bull. 41 (2008) 246.
[104] X. Feng, G. Yang, Q. Xu, W. Hou, J.J. Zhu, Macromol. Rapid Commun. 27 (2006) 31.
[105] R.J. Tseng, J. Huang, J. Ouyang, R.B. Kaner, Y. Yang, NanoLetters 5 (2006) 1077.
[106] J. Huang, S. Virji, B.H. Weiller, R.B. Kaner, J. Am. Chem. Soc. 125 (2003) 314.
[107] D.K. Moon, T. Maruyama, K. Osakada, T. Yamamoto, Chem. Lett. (1991) 1633.
[108] A. Ray, G.E. Asturias, D.L. Kershner, A.F. Richter, A.G. MacDiarmid, A.J. Epstein, Synth. Met. 29 (1989) 141.
[109] R. Kuhn, A. Wassermann, Ann. Chem. 503 (1933) 203.
[110] C. Walling, R.A. Johnson, J. Am. Chem. Soc. 97 (1975) 363.
[111] J. Weinstein, B.H.J. Bielski, J. Am. Chem. Soc. 101 (1979) 58.
[112] J.D. Rush, W.H. Koppenol, J. Am. Chem. Soc. 110 (1988) 4957.
[113] C. Sheu, A. Sobkowiak, L. Zhang, N. Ozbalik, D.H.R. Barton, D.T. Sawyer, J. Am. Chem. Soc. 111 (1989) 8030.
[114] J.H. Baxendale, Adv. Catal. (1952) 31.
[115] N. Toshima, H. Yan, M. Kajita, Y. Honda, N. Ohno, Chem. Lett. (2000) 1428.
[116] H. Yan, M. Kajita, N. Toshima, Macromol. Mater. Eng. 287 (2002) 503.
[117] A. Yasuda, T. Shimidzu, Polym. J. 25 (1993) 329.
[118] A.G. MacDiarmid, L.S. Yan, W.S. Huang, B.P. Humphrey, Synth. Met. 18 (1987) 393.
[119] P.N. Adams, P.J. Laughlin, A.P. Monkman, Polymer 37 (1996) 3411.
[120] F. Zhou, M. Angelopoulos, A.G. MacDiarmid, A.J. Epstein, Phys. Rev. B 36 (1987) 3475.
[121] Y. Cao, P. Smith, A.J. Heeger, Synth. Met. 55–57 (1993) 3514.
[122] N. Guskos, E.A. Anagnostakis, V. Likodimos, T. Bodziony, J. Typek, M. Maryniak, U. Narkiewicz, I. Kucharewicz, S. Waplak, J. Appl. Phys. 97 (2005) 024304.
[123] K. Suri, S. Annapoorni, R.P. Tandon, N.C. Mehra, Synth. Met. 126 (2002) 137.
[124] X. Yang, L. Xu, N.S. Choon, C.S.O. Hardy, Nanotechnology 14 (2003) 624.
[125] D.G. Shchukim, I.L. Radtchenko, G.B. Sukhorukov, Mater. Lett. 57 (2002) 1743.
[126] M. Wang, W. Li, J. Polym. Sci. 35 (1997) 2129.
[127] J.L. Dormann, D. Fioranim, Magnetic Properties of Fine Particles, North-Holland, Amsterdam, 1991, p. 309.
[128] M. Wang, W. Zhou, J. Li, Synth. Met. 78 (1996) 27.
[129] J. Deng, X. Ding, W. Zhang, Y. Peng, J. Wang, X. Long, P. Li, A.S.C. Chan, Polymer 43 (2002) 2179.
[130] Y.Z. Long, Z.J. Chen, Z.X. Liu, Z.M. Zhang, M.X. Wan, N.L. Wang, Chin. Phys. 12 (2003) 432.
[131] X. Lu, Y. Yu, L. Chen, H. Mao, H. Gao, J. Wang, W. Zhang, Y. Wie, Nanotechnology 16 (2005) 1660.
[132] H. Xia, D. Cheng, C. Xiao, H.S.O. Chan, J. Mater. Chem. 15 (2005) 4161.
[133] C. Yang, J. Du, Q. Peng, R. Qiao, W. Chen, C. Xu, Z. Shuai, M. Gao, J. Phys. Chem. B 113 (2009) 5052.
[134] H.P. Zhu, S.L. Mu, Synth. Met. 123 (2001) 293.
[135] Z.C. Sun, Y.H. Geng, J. Li, X.H. Wang, X.B. Jing, F.S. Wang, J. Appl. Polym. Sci. 72 (1999) 1077.
[136] P. Xu, A. Singh, D.L. Kaplan, Adv. Polym. Sci. 194 (2006) 69.
[137] W. Liu, J. Kumar, S. Tripathy, K.J. Senecal, L. Samuelson, J. Am. Chem. Soc. 121 (1999) 71.
[138] L.A. Samuelson, A. Anagnostopoulos, K.S. Alva, J. Kumar, S.K. Tripathy, Macromolecules 31 (1998) 4376.
[139] A.L. Cholli, M. Thiyagarajan, J. Kumar, V.S. Parmar, Pure Appl. Chem. 77 (2005) 339.
[140] K.G. Ryu, J.P. Mceldoon, A.R. Pokora, W. Cyrus, J.S. Dordick, Biotechnol. Bioeng. 42 (1993) 807.
[141] L.Z. Gao, J. Zhuang, L. Nie, J.B. Zhang, Y. Zhang, N. Gu, T.H. Wang, J. Feng, D.L. Yang, S. Perrett, X. Yan, Nat. Nanotechnol. 2 (2007) 577.
[142] Y. Wei, R. Hariharan, S.A. Patel, Macromolecules 23 (1990) 758.
[143] H. Xu, L. Cui, N. Tong, H. Gu, J. Am. Chem. Soc. 128 (2006) 15582.
[144] A.G. Roca, M.P. Morales, K. O'Grady, C.J. Serna, Nanotechnology 17 (2006) 2783.
[145] Y. Long, Z. Chen, J.L. Duvail, Z. Zhang, M. Wan, Physica B 370 (2005) 121.
[146] A.G. Roca, J.F. Marco, M. del Puerto Morales, C.J. Serna, J. Phys. Chem. C 111 (2007) 18577.
[147] J. Alam, U. Riaz, S. Ahmad, J. Magn. Mater. 314 (2007) 93.
[148] W. Xue, K. Fang, H. Qiu, J. Li, W. Mao, Synth. Met. 156 (2006) 506.
[149] X. Li, J. Shen, M. Wan, Z. Chen, Y. Wie, Synth. Met. 157 (2007) 575.
[150] N. Toshima, J. Tayanagi, Chem. Lett. (1990) 1369.
[151] Z. Zhang, M. Wan, Y. Wei, Nanotechnology 16 (2005) 2827.
[152] H.V.R. Dias, M. Fianchini, R.M.G. Rajapakse, Polymer 47 (2006) 7349.
[153] M. Salmon, K.K. Kanazawa, A.F. Diaz, M. Krounbi, J. Polym. Sci. Polym. Lett. Ed. 20 (1982) 187.
[154] P. Atkins, J. de Paula, Physical Chemistry, 7th ed., Oxford University Press, 2002.
[155] N.H. Dryden, J.J. Vittal, R.J. Puddephatt, Chem. Mater. 5 (1993) 765.
[156] A.F. Diaz, K.K. Kanazawa, G.P. Gardini, Chem. Commun. (1979) 635.
[157] D. Zhang, Polym. Test. 26 (2007) 9.
[158] S. Machida, S. Miyata, A. Techagumpuch, Synth. Met. 31 (1989) 311.
[159] N. Toshima, O. Ihata, Synth. Met. 79 (1996) 165.
[160] N. Ohno, N. Toshima, Chem. Lett. (1999) 435.
[161] A. Kotwal, C.E. Schmidt, Biomaterials 22 (2001) 1055.
[162] J.Y. Lee, C.A. Bashur, A.S. Goldstein, C.E. Schmidt, Biomaterials 30 (2009) 4325.
[163] T. Kessler, A.M. Castro Luna, J. Solid State Electrochem. 7 (2003) 593.
[164] S. Radhakrishnan, A. Adhikari, J. Power Sources 155 (2006) 157.
[165] G.M. Do Nascimento, V.R. Constantino, R. Landers, L.A. Marcia, Macromolecules 37 (2004) 9373.
[166] K. Mallick, M. Witcomb, M. Scurrel, A. Strydom, J. Phys. D: Appl. Phys. 42 (2009) 095409.
[167] H. Chang, Y. Yuan, N. Shi, Y. Guan, Anal. Chem. 79 (2007) 5111.